

Explaining accretion rates:

The effect of storms on vertical accretion rates of salt marshes on back barrier islands in the Dutch Wadden Sea



MSc thesis Wouter van der Niet

Hydrology and Environmental Hydraulics Group

Wageningen University

July 2025

Supervisors:

Dr.ir. RC (Roeland) van de Vijssel

Prof.dr.ir. AJF (Ton) Hoitink

Abstract

Salt marshes are important ecosystems, but they are at risk of drowning due to sea level rise. Vertical accretion through sedimentation during flooding is crucial in preventing the drowning of salt marshes. Most of this vertical accretion on salt marshes occurs during storms. Storm characteristics can drive vertical accretion by increasing suspended sediment concentration (SSC) through resuspension caused by elevated current and wave shear stress. However, both these mechanisms and the intra-marsh variability in storm impacts on accretion remain poorly researched.

In this study, we examine how storm characteristics relate to accretion rates in order to identify which storm factors have most influence on salt marsh accretion. Subsequently, we analyse storm effects over gradients such as the distance to the sediment source, which are known to play a role in accretion processes.

Yearly accretion rates on back-barrier salt marshes in the Dutch Wadden Sea are correlated to storm variables that are aggregated to a yearly resolution. Both the individual as well as the additive effect of storm variables on accretion rate are assessed through simple linear regression and multiple linear regression models respectively.

The results show that including most SSC-controlling variables offers little additional value compared to using only inundation-regime variables. This is because inundation depth during flooding is strongly correlated with many of the SSC-controlling variables. As a result, inundation depth alone captures most of the SSC dynamics on a yearly timescale and emerges as the key factor driving accretion rates. Conversely, the cross-shore wind speed is found to be independent of inundation depth and drives part of the accretion in addition to inundation-regime variables. It is expected that offshore winds provide high-SSC conditions and locally low-wave energy due to small fetch. This allows fast sediment settling, which increases accretion rates. Moreover, storms seem to govern the vertical accretion closest to tidal creek and shoreline, whereas accretion further from the sediment sources is thought to be governed by organic matter deposition.

Since the aggregation of storm variables into yearly data limits the temporal resolution, further research could benefit from analysis of SSC and storm variables at the resolution of individual storm events. In conclusion, this study highlights the dominant role of inundation depth and cross-shore wind in storm-driven accretion and underscores the spatial variability of these effects across salt marshes

Table of Contents

Introduction	7
Research objectives.....	10
Study area.....	11
Wadden Sea	11
Ameland	12
Schiermonnikoog.....	12
Methods	13
Processes captured by SEB measurement.....	14
Explanatory variables and data aggregation	15
Flooding regime variables	17
SSC-controlling variables	18
Regression analyses	19
Linearity.....	19
Correlation matrix	20
Multiple linear regression.....	20
Spatial analysis	22
Results	23
Simple linear regression	23
Correlation matrices	24
Multiple linear regression.....	26
Ameland	26
Schiermonnikoog	28
Spatial analysis	29
Discussion	32
Wave height	32
Long-shore wind speed and absolute wind speed	32
Cross-shore wind speed.....	33
Storm surge height.....	34
Inundation frequency and duration	34
Inundation depth	35
Spatial variability of storm-induced accretion	35
Difference between Ameland and Schiermonnikoog	36
Future Research Recommendations	37
Conclusion.....	40
References.....	41

Acknowledgements.....	46
Appendix 1: Cumulative aggregation method	47
Appendix 2: Varying inundation depth threshold analysis	50
Appendix 3: Analysis on period before inundation for SSC-variables.....	52
Appendix 4: Analysis on drivers of intra-marsh variability of impact of storm characteristics on accretion rate	55

Introduction

Salt marshes are valuable ecosystems which provide habitat for a large variety of species (Barbier et al. 2011). Next to biodiversity, salt marshes also play a critical role in flood defence (Temmerman et al. 2013), pollutant remediation and nutrient recycling (Barbier et al. 2011). Worldwide, salt marshes face the threat of drowning due to relative sea level rise (RSLR). Because of global warming, many parts of the world experience sea level rise (Cazenave & Cozannet 2014). Additionally, deep soil subsidence due to anthropogenic extractions (e.g., gas, salt and groundwater) occurs widespread (Couvillion et al. 2013; Kennish 2001). RSLR is the combined effect of sea level rise and soil subsidence. Because of the vital importance of salt marshes, it is crucial to research the impact of RSLR on their resilience.

RSLR poses a unique challenge to salt marsh ecosystems, as their vegetation depends on a delicate balance of flooding conditions to thrive (Costa et al. 2003). Salt marsh pioneer vegetation consists of halophytes, salt-tolerant plants uniquely adapted to grow under regular flooding conditions. Therefore, the salt marsh ecosystem relies on a specific frequency of flooding. If salt marshes are flooded less frequently, succession will take place and halophytes are outcompeted by species that are better adapted to fresher water (Castillo et al. 2021). The salt marsh will develop into a different type of ecosystem. On the other hand, if salt marshes are flooded more frequently and for longer durations, the vegetation will eventually die off. This is exactly the threat posed by RSLR.

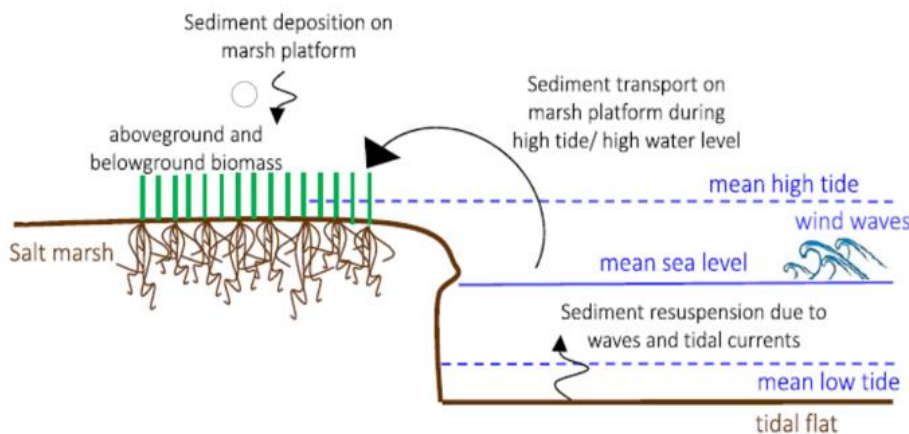


Figure 1: conceptual model of sediment accretion on salt marshes. Wind waves and tidal currents cause sediment resuspension. When the water floods the salt marsh, sediment settles and is deposited on the salt marsh. Adapted from Leonardi et al. (2017).

RSLR can be counteracted by vertical accretion of the salt marsh. Vertical accretion can be split into minerogenic accretion and organic matter accretion. It depends on the specific salt marsh whether organic matter or minerogenic accretion is dominant (Turner et al. 2001). This study focuses on salt marshes dominated by minerogenic accretion, which is driven by flooding (fig. 1). When salt marshes are flooded, the water is slowed down by the vegetation, creating favourable conditions for deposition of the sediments suspended in the water. After inundation, a thin layer of sediment is left behind, creating a small increase in elevation. The thickness of the newly deposited sediment layer is mostly determined by the depth of the water column flooding the salt marsh, the flood duration, the suspended sediment concentration (SSC) in the water, the vegetation density and marsh geometry (Butzeck et al. 2015; Drexler et al. 2019; Cornacchia

et al. 2024). Thus, accretion potentially allows salt marshes to grow with SLR, but it strongly depends on a complex combination of factors as discussed hereafter.

Although accretion is influenced by a complex interplay of factors and exhibits significant variability within marshes, a large portion - or even the majority - of accretion is induced by storms (Schuerch et al. 2011; Tognin et al. 2021; Cortese et al. 2024; Tognin et al. 2025). Understanding how storms affect accretion is therefore essential to explain temporal variations in sedimentation on salt marshes.

Storms influence accretion in two ways: through controlling the water level as well as the suspended sediment concentration (SSC). Wind setup can cause extreme water levels during storms, which flood the salt marshes. Because the inundation depth as well as the inundation duration are high, there is more sediment able to settle on the marsh. Moreover, a larger area of the salt marsh is inundated during extreme floods, so the spatial extent of accretion is larger. Both effects show that storms influence accretion just by increasing water levels.

In addition to flooding, storms also influence suspended sediment concentration (SSC), which is a critical factor in controlling accretion rates (Duvall et al. 2019; Panozzo et al. 2023). In simple terms, without sediment in the water, vertical accretion cannot occur. Understanding the factors that control SSC is therefore essential. SSC is controlled by resuspension processes, occurring when bed shear stress (τ_b) exceeds the critical bed shear stress (τ_{cr}). Bed shear stress results from two hydrodynamic forces: currents and waves. Current-induced bed shear stress (τ_c) scales with near-bed flow velocity (U) and is typically dominant in tidal channels and is given by Soulsby 1997 as:

$$\tau_c = \rho \cdot C_f \cdot U^2 \quad (1)$$

Where ρ is the water density and C_f the dimensionless bed friction coefficient.

Wave-induced bed shear stress (τ_w) depends on the near-bed orbital velocity (u_b) and is dominant in shallow waters such as tidal flats.

$$\tau_w = \frac{1}{2} \cdot f_w \cdot \rho \cdot u_b^2 \quad (2)$$

$$u_b = \pi H_s / (T \cdot \sinh(kh)) \quad (3)$$

Where:

- f_w = wave friction factor
- H_s = significant wave height
- T = wave period
- h = water depth

During storms, bed shear stresses are controlled by several storm-induced processes, which are governed by storm characteristics such as wind speed, wave height and storm surge. Typically, high wind speeds are present, which causes an increase in wave height. Wave height directly increases wave orbital velocity (eq. 3) which, in turn, quadratically increases the wave-induced shear stress (eq. 2). The wind direction is also a key factor and can be split in two components with different effects. Firstly cross-shore winds determine the fetch over which the wave height increases. For example, in the Danish Wadden Sea, it is found that high SSC occurs during strong onshore winds (the direction of the longest fetch) (Christiansen 2006). Secondly, long-shore winds cause long-shore sediment transport which can cause an import or export of suspended sediment (Ganju et al. 2013).

In addition to wave generation, wind stress also causes a setup of the water level known as storm surge. This wind setup increases hydraulic gradients and therefore increases tidal flows and ultimately current-induced bed shear stress in tidal channels. The meteorological impact on the water level is called the storm surge height. Next to wind speed, the storm surge height depends on a complex interplay of wind direction, atmospheric pressure, bathymetry and morphology (Lyddon et al. 2018). It is known however that storm surge increases linearly to quadratically with (south-)westerly wind speeds in the Wadden Sea (Gerkema & Duran-Matute 2017; Andrée et al. 2022). These mechanisms imply that current-induced and wave-induced shear stress are high during storm surges.

A final factor linking SSC and accretion is the settling velocity of suspended sediment during salt marsh inundation. Settling is influenced primarily by turbulence in the floodwater. Dense vegetation reduces turbulence and enhances sediment deposition (Duvall et al. 2019), while high wave energy keeps sediment in suspension and reduces deposition. On-shore winds thus have a dual effect: onshore winds increase SSC by increasing wave height, but they also inhibit deposition through increased bed shear stress (Duvall et al. 2019).

While the physical processes described above suggest a clear role for storms in accretion, it is important to examine whether such mechanisms are reflected in observed accretion patterns. Several studies found significant effects of storms on accretion rates. Tognin et al. (2021) find that the mean water depth during inundation has an exponential relation with accretion rate: the highest water levels, occurring during storm conditions, cause the most accretion. Schuerch et al. (2011) find that accretion rate correlates linearly with both flooding frequency and inundation depth, a proxy for storm intensity. Additionally, Van Dobben et al. (2022) use accretion rates on salt marshes in the Dutch Wadden Sea to study the relation between accretion and inundation depth and find similar to Schuerch et al. (2011), that flood frequency and inundation depth are significantly positively related to accretion rates. From this research it is clear that accretion rates increase with inundation frequency and inundation depth.

However, the storm variables discussed above primarily address the flooding regime, but storms also influence accretion through SSC. The direct relationship between storm characteristics and vertical accretion rates remains understudied. Specifically, how storm characteristics control accretion of salt marshes in addition to the already well-researched effect of the inundation regime variables (inundation depth and inundation frequency) remains to be studied. This represents the first knowledge gap that this study aims to address.

The Wadden Sea provides an ideal setting to study these relationships as it is a back-barrier tidal system subject to both natural and anthropogenic pressures. These include gas extraction and coastal engineering, which contribute to subsidence and accelerate the effects of relative sea level rise. Moreover, the Wadden Sea is a well-researched area with good data availability. The combined natural and human-driven processes, together with accessibility of long-term observational data, make it a relevant and suitable system for investigating the drivers of salt marsh accretion.

Physically, the Wadden Sea is characterized by large tidal flats and relatively sheltered salt marshes on back-barrier islands. In the Danish Wadden Sea tidal flat resuspension is the main source of SSC (Christiansen et al. 2008). Based on this context, we hypothesize that most accretion occurs during storm surge events with offshore wind directions that create long fetch and high waves on the tidal flats (enhancing SSC), while wave heights remain low over the marsh itself (favouring deposition).

A second knowledge gap is the spatial variability of storm-driven accretion. Accretion is further complicated by the spatial dynamics of accretion. Generally, the further from the sediment source, the lower the accretion rate (Butzeck et al. 2015). The sediment source in this case is the point in sea which has the shortest pathway through the tidal creeks to a specific point on the salt marsh. Close to tidal creeks, accretion rate is highest because this is inundated first when the water still contains a high SSC. The further from the tidal creek, the more sediment has fallen out of suspension and the less sediment is deposited. Furthermore, the length through the creek is relevant as further into the marsh, the SSC of the water in the tidal creeks drops (Temmerman et al. 2003; Bartholdy et al. 2010). Lastly, the elevation of the salt marsh determines how often the salt marsh is inundated. A lower elevation results in higher flooding frequency, meaning higher accretion rates. Thus, the spatial distribution of accretion rates is determined by the length through the creek, the distance to a tidal creek and the elevation of the salt marsh. During storms the tidal creek transport may be less important as extreme water levels cause a total overflow of the marsh where water from the sea can directly enter the marsh (Duvall et al. 2019). In this case it is expected that storms impact accretion rate more in areas on the salt marsh located further from the sediment source, because these areas are predominantly inundated during storms.

In summary, studies have shown that storms are the main driver of accretion. However, previous research has predominantly focused on storm-driven flooding regime characteristics, which is why this study aims to identify how storm-driven SSC dynamics contribute to vertical accretion rates of salt marshes on back-barrier islands in the Wadden Sea. Secondly, the intra-marsh variability of storm effects on accretion is underexplored. The goal is to explore whether empirical relations between storm characteristics and accretion rates can be identified, which can serve as physically meaningful indicators of the dominant accretion processes. By improving our understanding of the controls on salt marsh accretion rates this study contributes to assessing the resilience of these valuable ecosystems in the face of RLSR.

Research objectives

The objective of this study is to determine the extent to which SSC-controlling storm characteristics contribute to the vertical accretion rate of salt marshes. Linear regression models are used to correlate storm variables to long-term accretion rates recorded on two back-barrier salt marshes in the Dutch Wadden Sea. Additionally, the spatial differences in the effect of storm variables on accretion rates are addressed. Previously, linear regression models have proven useful in explaining long-term accretion rates using aggregated storm variables (Schuerch et al. 2011, Van Dobben et al. 2022). By completing the objectives this study contributes to a better understanding of vertical accretion rates on salt marshes

To complete the objectives, the following research questions are addressed:

Research questions:

1. How do SSC-controlling variables contribute to vertical accretion rates compared to flooding regime variables?
2. How does the relative contribution of SSC-controlling variables and flooding regime variables on accretion vary spatially within marshes?

Study area

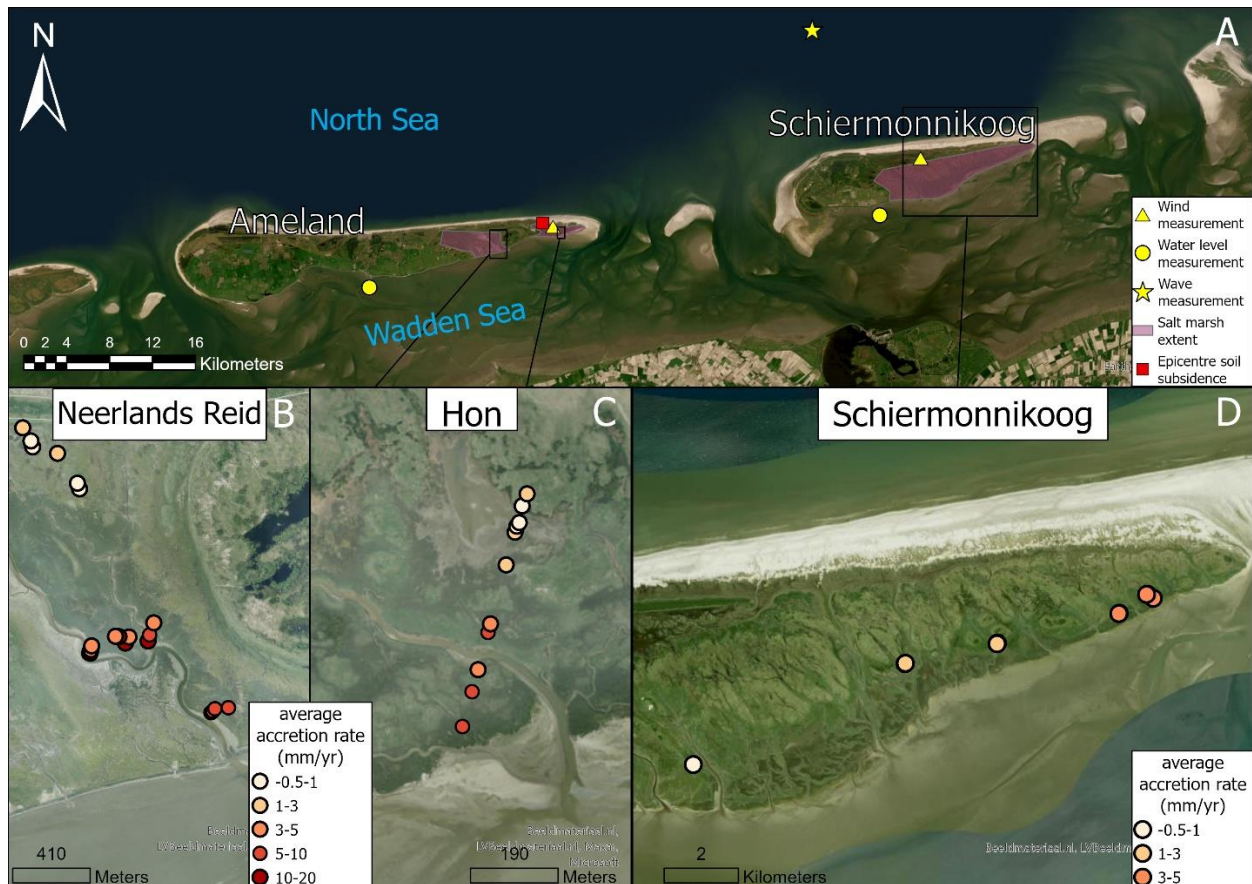


Figure 2: Maps of study area. (A) overview of measurement stations and study area. (B,C &D) Salt marshes on Ameland (B&C) and Schiermonnikoog (D) with average accretion rates of Sedimentation-Erosion Bars (SEB).

The study area consists of the back-barrier islands Ameland and Schiermonnikoog in the Dutch Wadden Sea (fig. 2A). Specifically, the salt marshes on the two islands are of interest.

Wadden Sea

The islands of Ameland and Schiermonnikoog are located in the Wadden Sea. The Wadden sea is a large intertidal area with tidal range varying between 1.4 and 3.4 meters. Due to a longshore current that is directed to the east, the back-barrier islands have been extending eastwards. This results in a chronosequence of the age of the salt marshes on the back-barrier islands. Salt marshes become younger in eastward direction on the islands. On both islands, the eastern part consists of salt marshes and the western part is older and endiked. The salt marshes have a clay layer with a maximum thickness of 80 cm, sitting on top of a sand layer (De Groot et al. 2011). The thickness of the clay layer is known to increase with age of the salt marsh, which is why there is a general trend of a thinning clay layer in eastward direction. Average clay thickness also differs between Schiermonnikoog (10 cm) Hon salt marsh on Ameland (15 cm) and Neerlands reid salt marsh on Ameland (50 cm).

Ameland

Ameland has a tidal range of around 2.2 meters. Mean high tide (MHT) is 1.0 meter above NAP (Dutch ordnance level representing mean sea level) (Van der Lugt et al. 2020). On Ameland natural gas extraction has been taking place since 1986. As a result, deep soil subsidence has occurred since 1986 and is still taking place (Van der Lugt et al. 2020). The epicentre which located on the Northwestern boundary of the Hon salt marsh (fig. 2) has subsided with 42 cm in the period 1986-2020 (NAM 2023). It is expected that soil subsidence will continue until the expected exploitation stop in 2050 (De Vlas 2017). On East-Ameland there are two salt marshes: Neerlands Reid and Hon, which are separated by an old dune formation called Oerderduinen (fig. 2).

Neerlands Reid (NLR) (fig. 2 and 3) started development around 1890. Several creeks are present that transport water and sediment in and out of the salt marsh with each tidal cycle. Neerlands Reid is located west of the subsidence epicentre (fig.1a). The total subsidence from 1986 until 2020 ranges from 4 to 26 cm increasing from west to east (NAM 2023). Neerlands Reid is used for grazing of livestock, which is known to be a source of compaction (Elschot et al. 2023). According to accretion measurements, Neerlands Reid is keeping up with RSLR near the salt marsh edge and near the banks of creeks, but further away from sediment sources, accretion is not keeping up with RSLR (Van Puijenbroek et al. 2024). In 1999, protection in the form of rocks was installed along the entire salt marsh edge except the eastern end near the Oerderduinen. This has kept the salt marsh edge of the Neerlands Reid in place since then.

The Hon (fig. 2) is a younger salt marsh which started to develop around 1960. It is located closer to the epicentre of subsidence, so more subsidence occurred here in the period 1986-2020 ranging from 26 to 38 cm (NAM 2023). Like Neerlands Reid, vertical accretion of the Hon keeps up with relative sea level rise only in parts of the marsh close to the sediment source. Further away from the sediment source the salt marsh is slowly sinking (Van Puijenbroek et al. 2024). There is no grazing by cattle and there is no salt marsh edge protection installed. This means the salt marsh edge is naturally retreating and expanding over time. Currently the eastern part of the Hon is expanding seaward, and the western part is retreating (Van Puijenbroek et al. 2024).

Schiermonnikoog

Schiermonnikoog is the back-barrier island east of Ameland (fig.4). On the east part of the island a salt marsh is present. Marsh age decreases from 200 years in the west to newly developing in the east (De Groot et al. 2011). Mean tidal range is 2.3 meter and MHT is around 1.0 meter above NAP. No gas extraction has taken place here, so deep soil subsidence is negligible. Vertical accretion measurements show that the salt marsh is accreting faster than sea level rise (Van Dobben et al. 2022). Cattle is present only on the most western part of the Schiermonnikoog salt marsh.

Methods

To determine the relationship between accretion rates and storm characteristics, data on sediment accretion and storm-related variables were analysed. Explanatory variables were divided into two categories based on their theoretical impact on accretion. Flooding regime variables were based on water level data and SSC controlling variables were based on water level, wave and wind data. After defining all the variables, a multiple linear regression (MLR) was performed with the accretion rates of each separate Sedimentation Erosion Bar (SEB) as dependent variable. The MLR approach allowed for the combined effect of the flooding regime variables and SSC-controlling variables to be assessed, resulting in statistical models that contained the set of storm variables that best explained the accretion rates. Finally spatial patterns in the correlations of both the flooding regime variables and the SSC-controlling variables to accretion rates were analysed.

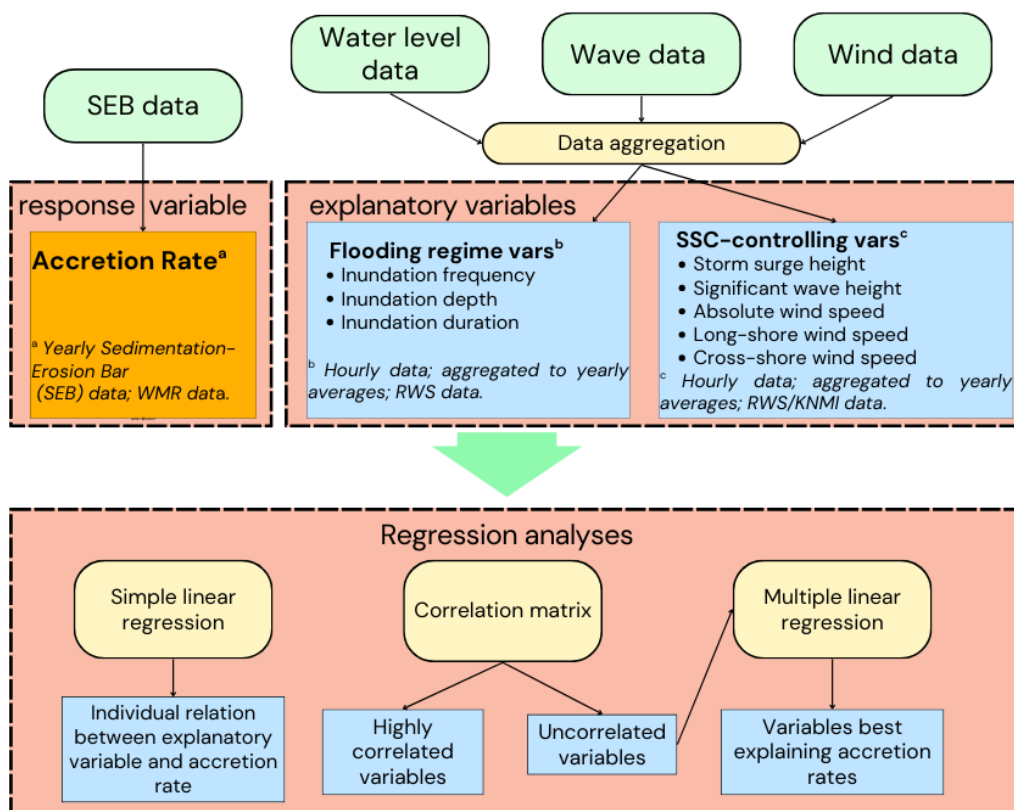


Figure 3: Flow chart outlining the methodology: from input data (top), to the definition of explanatory and response variables (middle), and finally to the implementation of regression analyses (bottom).

To investigate the relationship between accretion rates and storm characteristics, accurate measurements of elevation change were essential. In this study, SEBs were used to quantify accretion and erosion processes across salt marshes. The SEB measurement network included 24 stations on Ameland and 12 on Schiermonnikoog. Each SEB comprised two poles driven at least 1 meter into the ground (Nolte 2013). A 2-meter bar was placed between the poles, and measurements were taken at 17 equally spaced points with millimetre precision. By averaging the distance to the surface over the 17 holes the measurement had a sub-millimetre precision. (See Nolte 2013 for more detailed documentation on SEB).

Due to the different origin of the measurement plan, the SEB's on Schiermonnikoog were slightly different than the ones on Ameland. The SEB's on Schiermonnikoog consisted of 3 poles instead of 2 poles which formed a triangle between which the bar was placed. This resulted in 3 times 17 measurements per SEB which were averaged. Another difference is the spatial distribution of the SEBs: On Ameland they were structured in transects perpendicular to the shoreline (fig 2B), whereas the Schiermonnikoog SEB's were gathered in groups (fig. 2C). The SEB dataset contained yearly measurements from 1994 up to and including 2023, with some SEBs starting a few years later and sometimes missing a measurement. The measurements were taken at the end of summer or beginning of autumn by Wageningen Marine Research and further details on the measurement network were described by Elschot et al. (2017) and Van Puijenbroek et al. (2024).

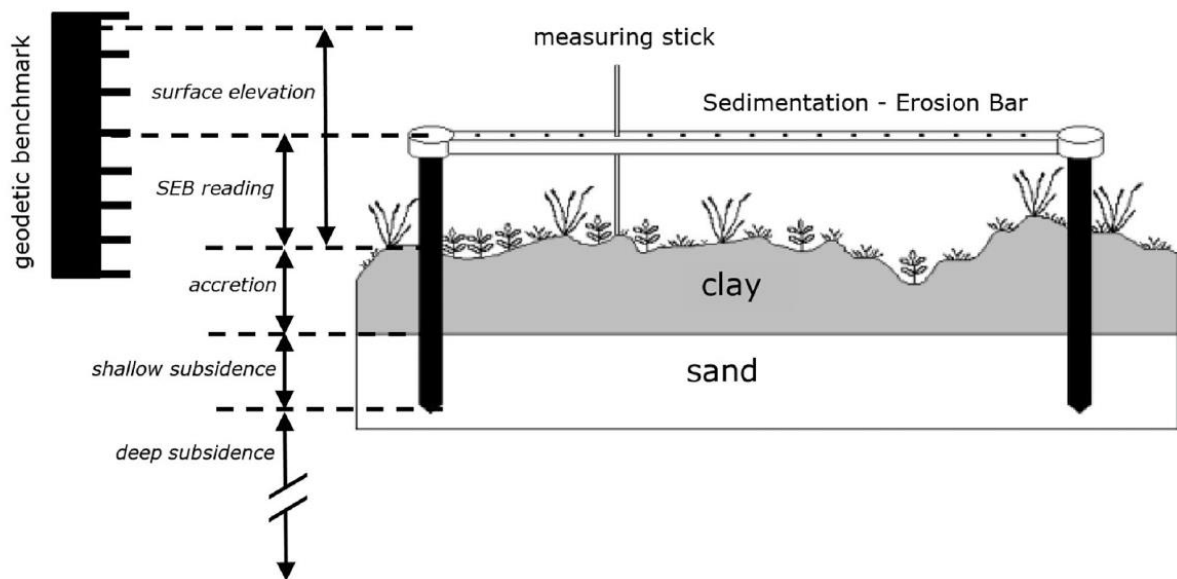


Figure 4: Diagram of a sedimentation-erosion bar (SEB). The bar is removed after measurements. The poles are permanent. Adapted from Dijkema et al. (2011) & Van Dobben et al. (2021).

Processes captured by SEB measurement

SEBs did not measure the isolated effect of accretion, but they rather measured the net vertical change of the entire clay layer, since the SEB poles are anchored in the stable sand layer below the clay layer. The vertical extension or shortening of the clay layer was the net effect of:

1. Swelling and shrinking due to changing soil moisture conditions (Van Wijnen & Bakker, 2001).
2. Autocompaction. The clay layer compacted under its own weight. There is more autocompaction on younger marshes and on marshes with thicker clay layers (Van Dobben et al. 2022).
3. Additional compaction by cattle (Elschot et al. 2023).
4. Sedimentation or erosion.

Van Dobben et al. (2022) did a statistical analysis on part of the same SEB dataset as used in this study and did not find a significant effect of autocompaction and the presence of cattle on the SEB measurements. As a result, these processes were assumed negligible in this study.

However, moisture conditions in combination with the thickness of the clay layer did have a significant effect on the SEB measurements. The effect of swelling and shrinking was not as significant as the flooding regime variables (Van Dobben et al. 2021). This, in combination with the complexity of adding a moisture balance to the salt marsh was why the moisture conditions

and clay thickness were not taken into account in this study. Therefore, the swelling and shrinking can be a source of noise in the data. Thus, in this study it was assumed that the difference in subsequent SEB measurements directly translated to accretion, which was divided by the length of the period between the two measurements to obtain the accretion rate. The accretion rate was used as the response variable in the multiple linear regression models. Since the accretion rate represented close to a full year, the explanatory variables which are defined in the next sections all had to represent the same period.

An inundation event was observed when the water level exceeded the elevation of the SEB. Consequently, the inundation depth was obtained by subtracting the SEB elevation from the water level. This was done for each SEB individually. For this calculation to be accurate, the elevation of the SEB stations relative to NAP had to be known. At the installation of each SEB, the elevation relative to ordnance datum was measured using differential GPS, which had a vertical accuracy of 2 cm (Trimble, 2009). When there was no deep soil subsidence (such as on Schiermonnikoog), the elevation over time was obtained by simply adding the difference between two consecutive SEB readings to the previous elevation level. However, since the SEBs did not measure deep soil subsidence, the deep soil subsidence on Ameland was quantified separately using a subsidence model (NAM, 2017). Van Puijenbroek et al. (2024) subtracted the modelled soil subsidence from the previous elevation relative to ordnance datum to obtain the elevation of the SEB stations over time. The uncertainty introduced by the subsidence model was on the order of millimetres (NAM, 2017).

Explanatory variables and data aggregation

Explanatory variables described the factors that were assumed to influence accretion rates over time. These variables were grouped based on their theoretical mechanisms of influence: flooding regime variables and SSC-controlling variables. The flooding regime characterized how often and how deep the salt marsh was inundated. An inundation was observed when the water level exceeded the SEB elevation. The SSC-controlling variables were related to the meteorological and hydrodynamical conditions influencing the SSC of the water inundating the salt marsh as explained in the introduction. Table 1 presents an overview of all explanatory variables.

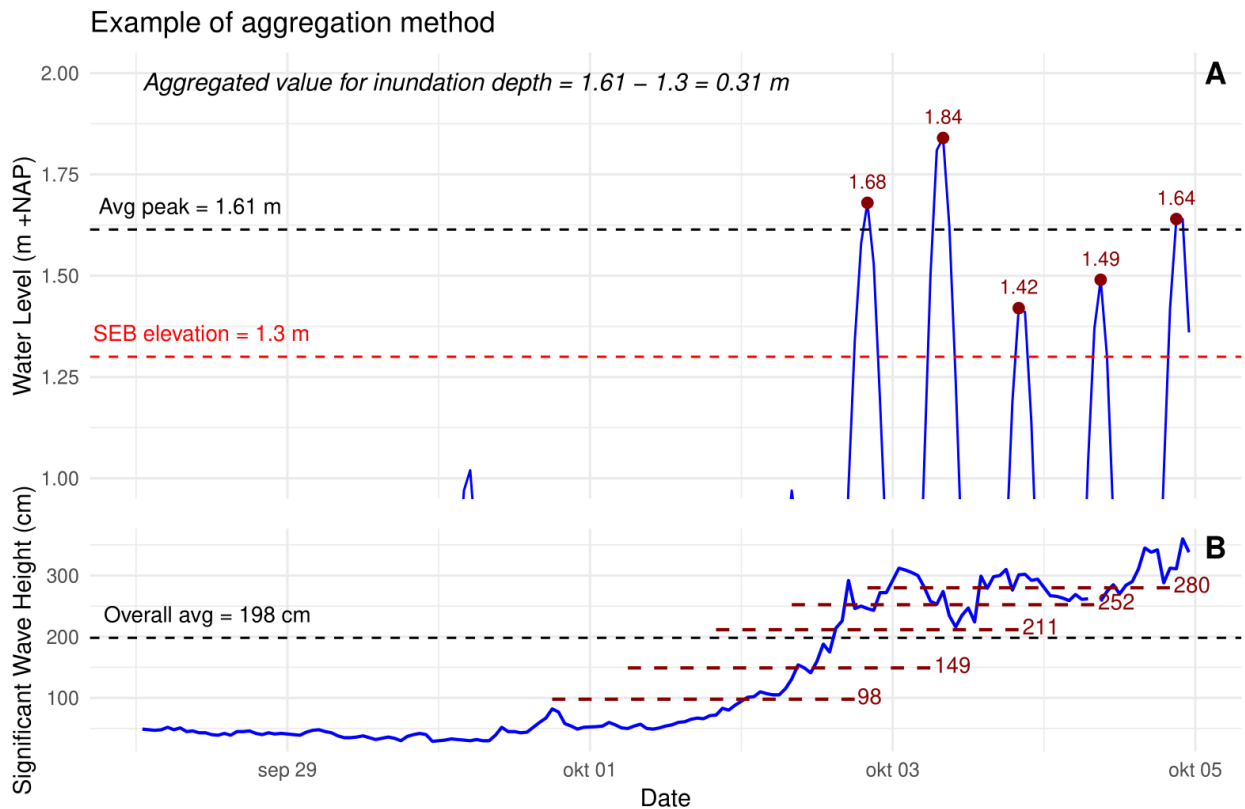


Figure 5: Illustration of aggregation methods. (A) timeseries of the water level during a one-week period. five inundations are observed, of which the peaks are averaged to obtain the aggregated maximum inundation depth during this period. (B) timeseries of significant wave height over the same one-week period. Averages of the 2-day period before the peak inundation level are averaged again to obtain the aggregated significant wave height during the one-week period.

For the regression analyses to work, explanatory variables must match the period covered by the accretion rate. Since the accretion rate values were calculated using two subsequent SEB measurements roughly one year apart, all explanatory variables must represent the same period of a year. We chose to aggregate all explanatory variables to one year by using the average of these variables over all inundation events in the corresponding period between two SEB measurements. The average was chosen because this way all events were taken into account. Aggregation by accumulation also includes all inundation events and was explored as well (appendix 1). The cumulative aggregation method resulted in a signal of the variables that was mostly determined by the inundation frequency during the year. So, this method was less suitable to compare the effect of the different storm characteristics as is the goal of this study.

Figure 5 explains the aggregation procedure, using a shorter (one-week) period for illustration purposes. Figure 5A shows how five peak inundation level were identified, which were averaged over the entire period to obtain one average peak inundation level. Finally, the SEB elevation was subtracted, which resulted in the aggregated value for inundation depth for this one-week period.

In this study, all inundation events were included in the aggregation of explanatory variables. Since storms were known to be major drivers of sediment accretion, a supplementary analysis was performed to assess whether focusing only on higher-inundation events (i.e., more intense

storms) would improve the model’s explanatory power (see Appendix 2). This pre-analysis, based on increasing inundation thresholds, showed no improvement in explaining accretion rate variability. Therefore, the decision to include all inundations was justified and maintained throughout the main analysis.

In figure 5B the significant wave height is plotted but the method was similar for the other SSC-controlling variables: an average of the 2-day period prior to each flood event was calculated. Afterwards, the average of all these values was calculated over the period between two subsequent SEB measurements. This resulted in one aggregated value for the entire period, which was used as input for the regression analyses.

Table 1: Overview of explanatory variables, their definitions and formulae. Note that all variables except inundation frequency were averaged over one year to match the period over which accretion was measured. Additionally, for the SSC-controlling variables, the average of the 2-day period before inundation was taken.

Explanatory variable	Definition	Formula
Flooding regime variables		
Inundation frequency	Frequency of inundations in the measurement period	Number of inundations in measurement period / length of period
Inundation depth	Maximum inundation depth during one inundation	
Inundation duration	Cumulative duration of inundations during aggregation period	Σ individual inundation durations / length of period
SSC-controlling variables		
Storm surge	Difference between actual water level and astronomically predicted water level	measured water level - astronomically predicted water level
Wave height	Significant wave height = mean of highest one-third of the waves measured from trough to crest	
Absolute wind speed	Absolute wind speed	
Cross-shore wind speed	Wind speed in cross-shore direction (offshore wind = positive)	$-1 \cdot v_{abs} \cdot \sin((\theta - \alpha) \cdot (\pi/180))$ With: v_{abs} = absolute wind speed (m/s) θ = wind direction (°) α = shoreline orientation (°)
Long-shore wind speed	Wind speed in long-shore direction	$-1 \cdot v_{abs} \cdot \cos((\theta - \alpha) \cdot (\pi/180))$

Flooding regime variables

Water level data at a 10-minute interval was provided by Rijkswaterstaat on the locations of Nes (Ameland) and Schier (Schiermonnikoog). The water levels were measured by tidal gauges, located within 15 km from all SEBs and within the same tidal basin as the SEBs, so difference in water level between the tidal gauge and SEBs was minimal. Two flooding regime variables were defined in this study, similarly to Schuerch et al. (2011): inundation frequency and inundation depth. Inundation frequency was defined as the number of inundations in a period divided by

the length of that period. Inundation depth was defined as the maximum water depth on the marsh during a flood event. Using these definitions, the variables were statistically independent from each other (Schuerch et al. 2011), which was important for the multiple linear regression. The last flooding regime variable was inundation duration, which was defined as the duration for which the salt marsh was inundated.

SSC-controlling variables

Storm surge is typically approximated by the residual water level, which is the difference between the astronomically predicted water level and the actual water level (Lyddon 2018). However, discrepancies between predicted and observed water levels may also arise from other sources, including inaccuracies in the tidal model. In this study, a 10-minute interval storm surge data series was produced. First, the astronomically predicted water level was calculated using the Utide package in MATLAB. Subsequently, the residual water level was calculated by subtracting the astronomical water level from the measured water level. Then a low-pass filter was applied to the residual water level which filtered out frequencies above 0.8 cycle/day to make sure remaining tidal components as well as wind waves and noise were removed. The filter was a frequency-domain filter making use of Fast Fourier Transform function. Lastly, the average storm surge height of the 2-day period before each inundation was calculated.

For all SSC-related variables, the period before the inundation starts must be considered, since the SSC *during* the inundation is determined by the storm conditions *before* the inundation. A 2-day period before the inundation was chosen in this study after analysis with simple linear regression between the accretion rates and the SSC variables, using time periods before inundation ranging from 0 (only the value at inundation peak) to 14 days (appendix 3). The analysis showed that the 2-day period was in most cases the period which resulted in the most significant relation between accretion and the explanatory variables. However, there was considerable variability in which period resulted in the best model across locations and variables. Therefore, while the 2-day period appeared to be a generally effective choice, it should not be considered definitively superior or universally optimal across all conditions.

Significant wave height at a 10-minute interval was provided by Rijkswaterstaat from 1994 to 2023. Significant wave height was defined as the mean of the highest one-third of the waves on the temporal domain. The measurement location was located 10 km north of Schiermonnikoog (fig. 2A), meaning the waves were measured at the North Sea rather than the Wadden Sea. The SEB's on Ameland and Schiermonnikoog were all located at a distance between 15 and 25 kilometres from the wave gauge. Therefore, wave height in this study represented fetch-unlimited settings, not the local wave conditions on the marsh.

As such, wave height should be interpreted as a proxy for regional sediment availability, primarily driven by resuspension on exposed tidal flats in the Wadden Sea or sediment advection from the North Sea, rather than local resuspension adjacent to the salt marsh platforms themselves. Importantly the sedimentation-inhibiting effect of local wave climate is not present in the wave height data.

Wind data was provided by the Royal Dutch Meteorological Institute (KNMI). The data was part of the KNMI North Sea Wind atlas (KNW-atlas) which contains hourly wind data based on more than 40 years of re-analysed data. They are not direct measurements but rather interpolations of measurements. According to KNMI the daily cycle of wind speed was not reproduced in the KNW data. However, wind data in this study was used for averages of at least two days, making the wind data representative. From the KNW-atlas the wind speed and direction at 10 meters height was extracted for two locations: one on the centre of the Ameland salt marshes and the other one on the centre of the Schiermonnikoog salt marshes. Both the absolute wind speed and the wind speed split in cross-shore and long-shore directions were used as explanatory variable. The wind speed in long-shore and cross-shore direction were calculated with the sine and cosine times the wind speed with positive directions according to figure 6. The shoreline orientation (i.e. the angle the shoreline makes with true north) is provided in Table 2. Note that for Schiermonnikoog, different shoreline orientations were used depending on the location of the SEB. Although shorelines change over time in a dynamic area as the Wadden Sea, this effect was considered negligible since the stretches over which the shoreline orientations were measured were at least one kilometre long. Therefore the shoreline direction used in this study were constant in time.



Figure 6: Schematic illustration of long and cross-shore positive wind directions.

Table 2: Shoreline orientations as measured clockwise from true north over stretches of at least one kilometre.

Salt marsh	Shoreline orientation (°)
Neerlands Reid	76
Hon	80
Schiermonnikoog	68-90

Regression analyses

To determine the extent to which each explanatory variable influences accretion rates, regression analyses were conducted. First, simple linear regression was applied to each SEB station to evaluate individual relationships between explanatory variables and accretion rates based on the Pearson correlation coefficients. The Pearson correlation coefficients are numbers between -1 and 1, where -1 is a perfect negative correlation, 0 is no correlation and 1 is a perfect positive correlation.

Linearity

Linear regression assumes there are only linear relationships between accretion and the explanatory variables. This is contradictory to what can be expected based on the non-linear physical and sometimes empirical relations between accretion, SSC, flooding regime and SSC-controlling variables observed by several studies (Tognin et al. 2021, Christiansen et al. 2006). However, these are studies on unaggregated data, meaning they cover timeseries of weeks or months, where SSC or accretion is measured in a higher frequency than once a year. The logical result is that those studies can find direct physical relationships between the discussed variables.

This study, however, aimed to characterize the long-term accretion of salt marshes with yearly accretion measurements, meaning that the aggregated data summarize conditions over an entire year. The result is that physical relations are represented in a more indirect way.

Other studies using aggregated storm variables to explain long-term accretion rates have shown that linear models describe the relation best (Schuerch et al. 2011, Van Dobben et al. 2022). The consequence of using aggregated variables is that direct isolated relations between accretion and the storm variables can not be identified. What the aggregated approach can identify which overall storm variables can explain long-term accretion rates best. By finding these variables, hypotheses on the mechanisms of accretion during storms could be formed. These can form the basis of detailed physically grounded studies.

The assumption of linearity was here verified in two ways:

1. By visual inspection of the scatterplots of each variable against the accretion rates. The scatterplots showed no significant non-linear trends, supporting the assumption of linearity.
2. By applying a general additive model (GAM), linearity of relations between explanatory and response variable, was checked. A GAM is a model that can apply smooth functions on the explanatory variables. The degree of smoothness is captured by the effective degrees of freedom (EDF) parameter. When EDF is approximately equal to 1, the relationship found is linear. After applying the GAM to the dataset, EDF was smaller than 1.01 for 95% of the relations found. The EDF's higher than 1.01 were all found on different locations with different explanatory variables. This indicated that there is no sign of a significant non-linear relation found in the data and justified the use of the multiple linear regression.

Correlation matrix

When applying MLR it is important to prevent collinearity of explanatory variables. Collinearity means that two variables are highly correlated to each other and therefore pass the same signal to the response variable. With a high degree of collinearity, it becomes hard to identify the variable that is truly driving the process as the found relationships are unreliable (Ahmad 2019). To check for collinearity all explanatory variables that were defined, were correlated to each other in a correlation matrix. Following Baaij et al. (2021) absolute Pearson correlation coefficient values of 0.6 or higher were considered too intercorrelated to use both in one MLR model.

Multiple linear regression

Finally, the MLR was applied to the dataset. Equation 4 shows how a MLR model uses the explanatory variables to predict the response variable, with y the response variable, accretion rate in this case, X_n an explanatory variable, and β_n the coefficient that addresses the effect of the explanatory variable on the response variable.

$$y = \beta_0 + \beta_1 X_1 + \dots + \beta_n X_n \quad (4)$$

The β -coefficients were of interest in this case as they contained the effect of each explanatory variable on the accretion rate. By comparing the β -coefficients, the variables with the most influence on accretion rate could be identified as well as possible underlying accretion mechanisms. To be able to compare the β -coefficients, they were made unitless by standardizing the timeseries of all the variables. Standardization means that each data point is

transformed to a unitless value by subtracting the mean and subsequently dividing by the standard deviation of the timeseries. The MLR was conducted on the standardized data, which did not affect the model's outcome except that the intercept (β_0) became zero.

To identify which combination of variables produced the MLR model explaining the accretion rates best, a variable selection method was applied. Backward selection selected variables starting by considering all variables in the model and then it iteratively removed the least significant variables until an optimal model was reached. Backward variable selection was chosen as the most suitable method considering the high number of explanatory variables (8 in this study) relative to the sample size (20-30 accretion measurements). The Akaike Information Criterion was chosen as the parameter to base the selection process on. The Akaike Information criterion aims to find a balance between the number of parameters in a model and the goodness of fit (MacDonald, 1989). The model with the lowest AIC is regarded as the best model. The backward selection procedure identified at each step how much the AIC would improve by dropping each variable and then it dropped the variable that would improve the AIC most. This process continued iteratively until dropping another variable resulted in a higher AIC than the previous model. The result was a model that incorporates the set of explanatory variables, which together best explain the accretion rate on salt marshes.

Finally, the p-value of the F-statistic was used to decide whether the final MLR model was significantly explaining the variation in accretion rates. The F-statistic is a parameter that indicates whether (at least one of) the explanatory variables fit the data better than a model without predictors. The p-value of the F-statistic can be used to test for significance of the model. In this case a significance threshold of 0.10 was used instead of the more usual 0.05 threshold because accretion rates are influenced by external factors such as vegetation dynamics, which is not accounted for in this analysis. Additionally, accretion rate measurements are subject to noise due to shrinking and swelling. Given this high variability, we opted for a slightly more lenient threshold to reduce the risk of overlooking meaningful relationships between storm variables and accretion rates.

Spatial analysis

Lastly, this study aimed at answering the question of how storm impact on accretion rates is distributed within marshes. First the direct dependency of accretion rate to spatial variables was identified by simple linear regression between accretion rates and the spatial variables. Spatial variables considered were distance to creek, distance to shoreline, distance to sediment source, elevation and vegetation height. The distance to creek and shoreline was determined on each SEB location by identifying the closest shoreline or creek from satellite maps in ArcGIS software (fig. 7). The distance to sediment source is the minimum distance to either creek or shoreline. Vegetation height and elevation were collected in-situ by Wageningen Marine Research together with the SEB measurements (Van Puijenbroek 2024). From the simple linear regression, it becomes clear what spatial variable is causing most spatial variability in the dataset.

Subsequently, the spatial dependency of accretion rate on storms was studied by plotting the correlation between the storm variables and accretion rates as a function of the spatial variables. The resulting plots were analysed to find patterns of how storm characteristics affect accretion over gradients of spatial variables. With this, it could be analysed which spatial variables (mostly related to marsh geometry) affect storm-induced accretion most and through which storm variable.

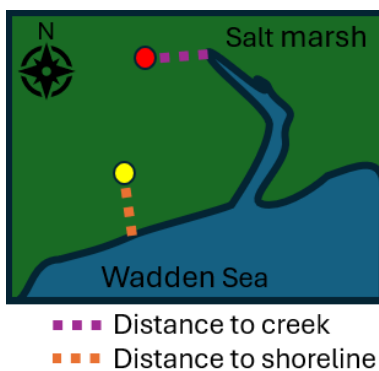


Figure 7: Schematic illustration of the spatial variables distance to creek and distance to shoreline. Dotted lines indicate shortest distance from a SEB (coloured dots) to a creek or shoreline, respectively.

Results

This section starts by examining the comparative explanatory power of the explanatory variables, focusing on whether incorporating SSC-controlling variables helps explaining accretion rates relative to flooding regime variables. Following this, the focus shifts to present spatial patterns in storm effects, using correlations between explanatory variables and accretion rates across spatial dimensions to identify location-specific trends and relationships.

Simple linear regression

The Pearson correlation coefficients of the simple linear regression between each individual explanatory variable and accretion rate are plotted for the SEB locations on Ameland in figure 8. The locations are ordered by increasing distance to the sediment source for both the Hon and Neerlands Reid (fig. 2), because distance to sediment source is a well-known driver of spatial variability (van Puijenbroek et al. 2024). The correlation coefficients range from -0.4 to 0.7 and most are positive correlations. An important observation is that the correlation between explanatory variables and accretion varies significantly across locations. None of the storm variables has the same correlation on all locations. When comparing between storm variables, there are some variables that show similar patterns. Firstly, the long-shore and absolute wind speed show a similar pattern. Secondly, inundation frequency and inundation duration show a similar pattern. In both cases this is because the variables are strongly intercorrelated as shown in figure 10.

On Neerlands Reid, the wind variables show the least consistency across the locations, being negative in one, and positive in the next locations. This is a first indication that the wind is an important driver of intra-marsh variability in storm-induced accretion. Storm surge, on the other hand, is most consistent with predominantly slightly positive correlations.

A comparison between flooding regime variables and SSC-controlling variables reveals an important pattern: wave height and storm surge have a similar influence on accretion as inundation depth.

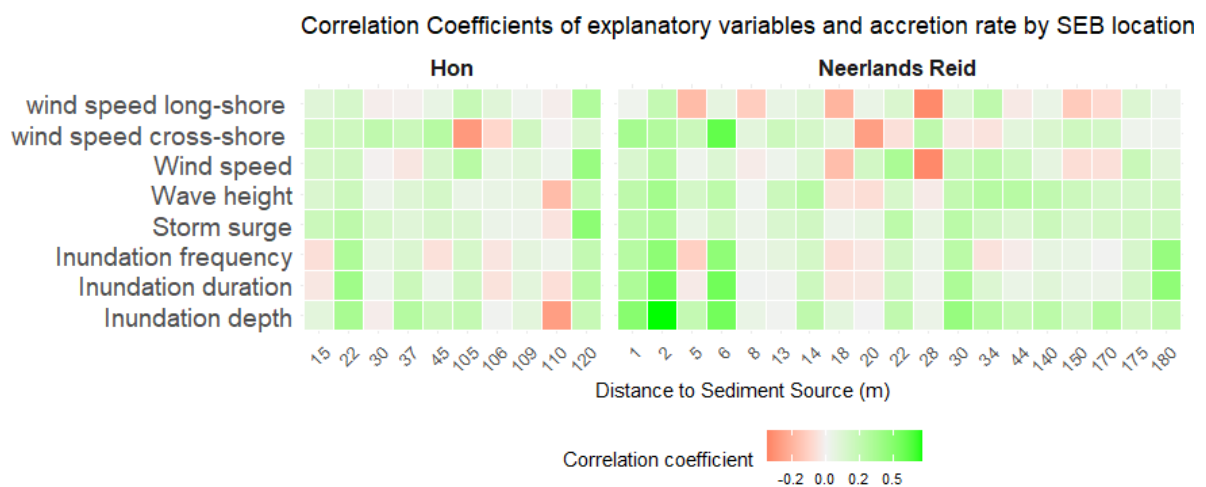


Figure 8: Pearson correlation coefficients of the simple linear regression between each explanatory variables and the accretion rate on each SEB on Ameland subdivided over the Hon and Neerlands Reid. The different SEB stations are represented on the x-axis by their distance to the sediment source.

On Schiermonnikoog the Pearson correlation coefficients range from -0.35 to 0.70 (fig. 9). Again, the SEBs are ordered according to the distance to the sediment source but the range of distance to sediment source is much smaller (28 to 82 m), so the influence of the distance to sediment source should be less, compared to Ameland.

In contrast to Ameland, the SEBs on Schiermonnikoog all show a very similar relation to the flooding regime variables. All flooding regime variables and storm surge have a relatively high positive correlation (around 0.5). Similar to Ameland, the wind variables show inconsistent behaviour between the SEB locations, where correlation can be positive or negative.

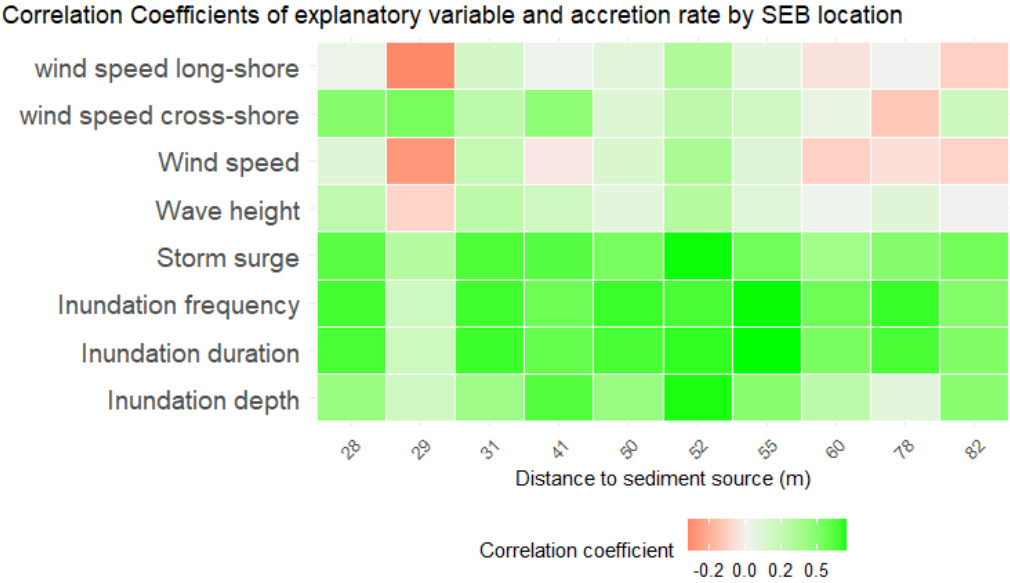


Figure 9: Pearson correlation coefficients of the simple linear regression between each explanatory variables and the accretion rate on each SEB on Schiermonnikoog. The different SEB stations are represented on the x-axis by their distance to the sediment source.

Correlation matrices

The correlation matrices show the Pearson correlation coefficients between all the explanatory variables on the aggregated data, which is the same as used for input for the correlation with accretion rate. Figure 10 and 11 representing Ameland and Schiermonnikoog respectively, clearly show that most of the SSC-controlling variables are highly positively correlated to each other. These variables are storm surge, wave height, wind speed and long-shore wind speed. Especially on Ameland the correlation between these SSC-controlling variables is very high ranging from 0.84 to 0.96. One of the conditions for applying MLR is that the explanatory variables are independent of each other. Therefore, the high collinearity between these variables is problematic for MLR, so only one of the SSC-controlling variables can be used for MLR. This is not the case for cross-shore wind speed as it shows low absolute correlations to the other variables, proving it is independent of the other variables, which is why it can be used in the MLR models in addition to one of the other SSC-controlling variables.

When comparing the SSC-controlling variables to the flooding regime variables, the correlation of the SSC-controlling variables with inundation depth is considerably high. This means that in a year with high mean inundation depth, the waves, (long-shore) wind and storm surge also tend to be more intense in that year. This is a key result as it would indicate that, when yearly aggregated values are considered, the added value of SSC-controlling variables in explaining

accretion rates is low because inundation depth covers the overall influence of SSC on accretion already.

On Schiermonnikoog the correlation of SSC-controlling variables with inundation depth is higher (0.57 to 0.66) than on Ameland (0.47 to 0.55). This has to do with the distribution of SEBs over different elevations. The SEBs on Ameland cover a wider range of elevations (fig. 15 and 16), thus also covering a wider range of mean inundation depths, which results in more scatter of the data, so less correlation.

On both Ameland and Schiermonnikoog, the inundation frequency and duration have the extremely high pairwise correlation of 0.99 and 0.98, respectively. This means that these variables carry the same signal. Because of the high correlation, the variables cannot both be included in the multiple linear regression. It was decided to only use inundation frequency as this variable is most often used in literature (e.g. Schuerch et al. 2011). The correlation of inundation frequency and duration to the SSC-controlling variables is strongly negative on Ameland and only slightly negative on Schiermonnikoog. This can be explained by the elevation difference. Schiermonnikoog has SEBs that are generally on higher elevation than Ameland (fig. 15 & 16). Lower salt marshes have a higher inundation frequency but the average storm during these inundations will be less severe, resulting in negative correlation between inundation frequency/duration and storm variables.

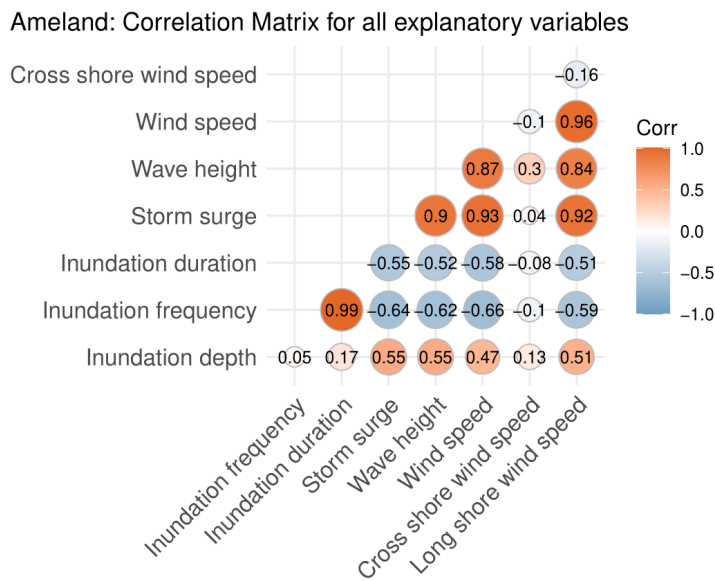


Figure 10: Correlation coefficients of all explanatory variables using the aggregated timeseries on Ameland.

Schiermonnikoog: Correlation Matrix for all explanatory variables

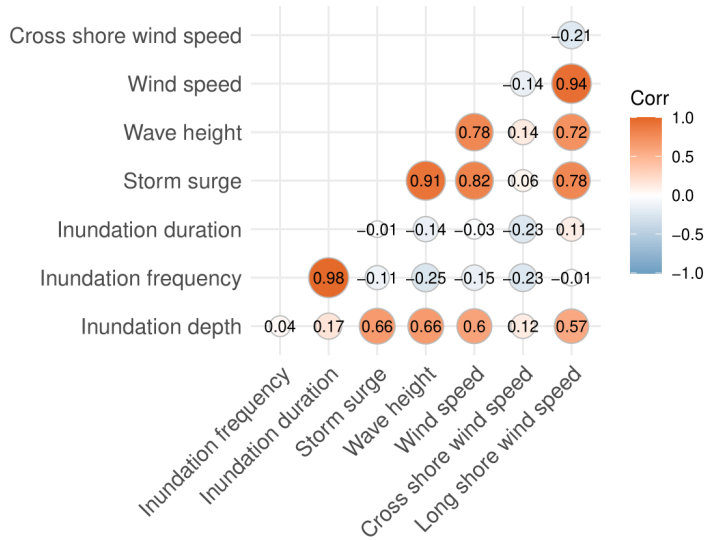


Figure 11: Correlation coefficients of all explanatory variables using the aggregated timeseries on Schiermonnikoog.

Multiple linear regression

Based on the collinearity found in the correlation matrices, a pre-selection of variables was made. Similar to Baaij et al. 2021, an absolute pairwise correlation higher than 0.6, was deemed too high to incorporate both variables in the MLR model. Mainly, the high intercorrelation between inundation depth, wave height, wind speed, storm surge height and long-shore wind speed is problematic. Because it is known that inundation frequency and inundation depth are crucial in determining accretion rate, it was chosen to include these in all models and expand the model with SSC-controlling variables that are not (too) collinear with the flooding regime variables. This means that on both islands inundation depth, inundation frequency and cross-shore wind speed were included in the pre-selection. On Ameland, the variables storm surge, wave height, wind speed and long-shore wind speed were incorporated one by one in different models because their intercorrelation is too high to include all of them at the same time. On Schiermonnikoog, the variables storm surge, wave height, wind speed and long-shore wind speed were totally excluded as their correlation to inundation depth was too high. The β -coefficients of the significant MLR models with varying explanatory variables are presented in figure 12 and 14. The final models that were insignificant according to the p-value of the F-statistic (> 0.10) are not presented.

Ameland

On Ameland, only 7 to 13 out of 29 SEB locations result in a significant model with the indicated set of preselected variables. The adjusted R^2 of the models ranges between 0.08 and 0.53 (fig. 13). In the first model where only inundation depth, frequency and cross-shore wind speed are incorporated, just two locations show a combination where all three variables are contributing to the explained variance. These are also the only two models where cross-shore wind speed contributes. Thus, on Ameland the cross-shore wind speed is not very important for accretion. In contrast, the inundation depth and frequency are significantly explaining accretion in more locations. The beta coefficients for inundation depth and frequency are mainly positive, which is in line with expectation as more and higher inundations would logically cause more accretion.

However, it is worth noting that the contribution of inundation depth and frequency is not significant in most of the locations on both the Hon and NLR.

Long-shore wind speed and storm surge height were selected more often in the final MLR model in the approaches in which these variables were added to the preselection. Especially long-shore wind speed seems very significant in this case. However, in 6 out of 8 locations where the long-shore wind speed was chosen it occurs together with inundation depth in a model, where inundation depth has a positive beta coefficient and long-shore wind speed has a negative beta coefficient. The negative beta coefficient is contradictory to the positive correlations found between long-shore wind speed and accretion rate in the simple linear regression in figure 8. This indicates that collinearity is causing the beta coefficients of long-shore wind speed to inflate and to be *falsely* selected as a significant predictor (Kim 2019). Lastly, wave height is only selected in one location as a significant predictor. Thus, overall wave height is not adding significantly to the explanation of variance in accretion rates on Ameland either.

β -values across MLR models with varying explanatory variables (Ameland)

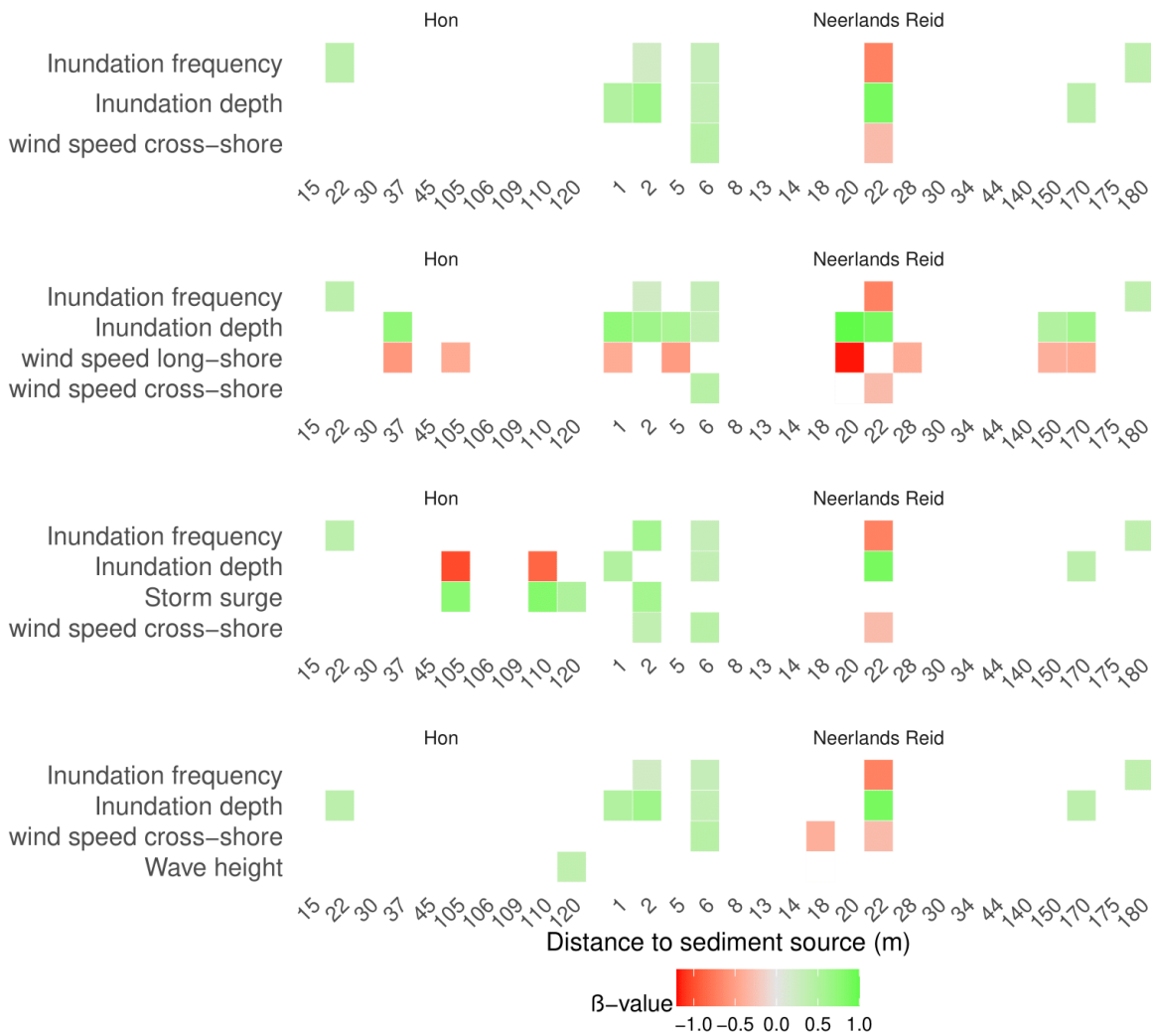


Figure 12: β -coefficients of 0.1 level significant multiple linear regression models plotted over distance to sediment source. Each subplot has a different set of SSC-controlling variables on which the AIC-based backward variable selection is performed to derive a significant MLR model.

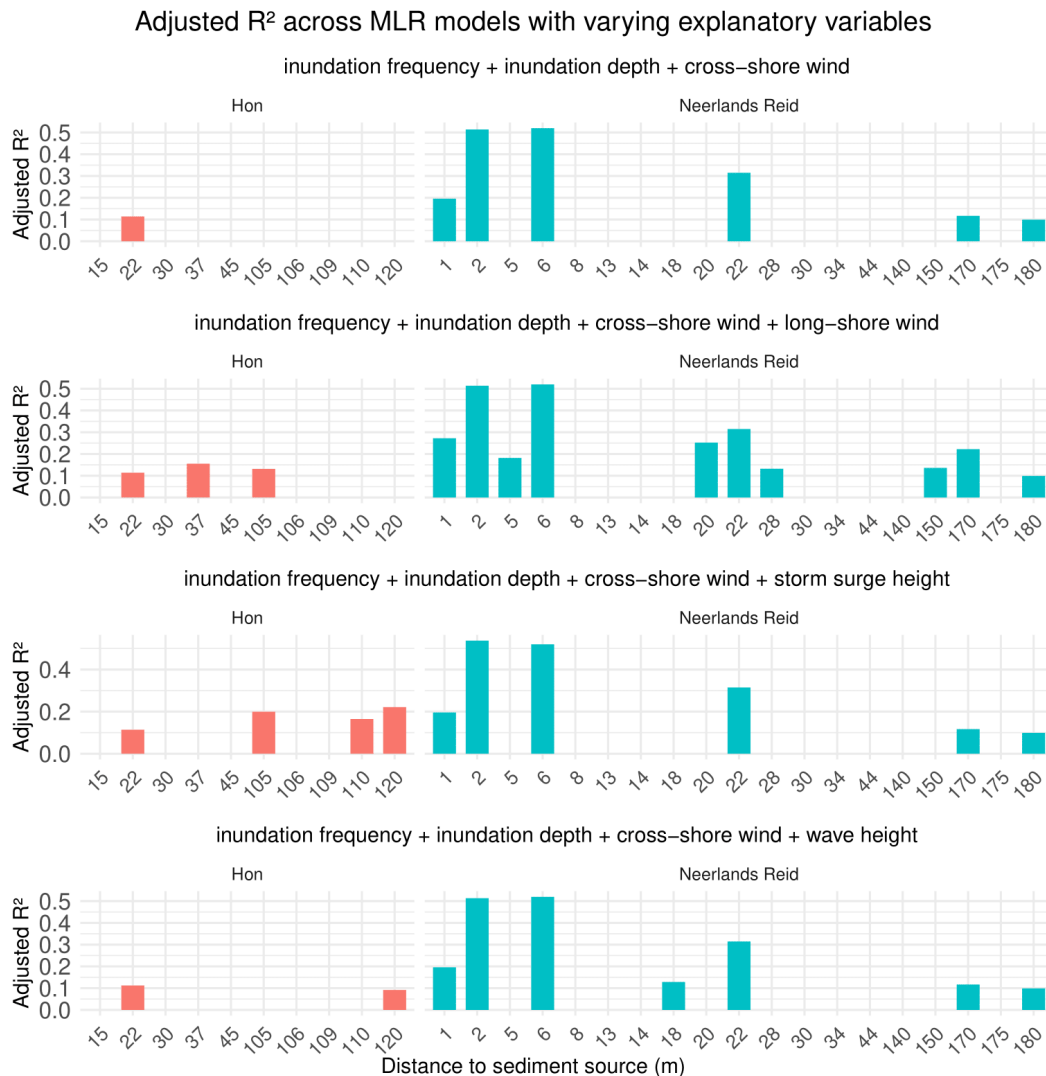


Figure 13: Adjusted R^2 values of significant MLR models with varying set of explanatory variables, corresponding to figure 12.

Schiermonnikoog

Seven out of nine SEB locations on Schiermonnikoog produces a significant model, which is a much higher fraction than for Ameland (fig. 14A). The adjusted R^2 of the MLR models ranges from 0.22 to 0.51 (fig. 14B). Inundation frequency and cross-shore wind speed contribute both to 6 out of 9 SEB locations, whereas inundation depth contributes to only 2 SEB locations. This is different compared to Ameland where inundation depth seems a more significant predictor of accretion than cross-shore wind speed.

All beta coefficients are positive, except one beta coefficient of inundation frequency that is negative. As shown in Figure 6, the positive direction of cross-shore wind speed corresponds to an offshore wind. Therefore, positive beta coefficients for cross-shore wind speed indicate that stronger offshore winds prior to inundation are associated with increased accretion rates on

Schiermonnikoog. This finding indicates that SSC-controlling variables can have added value to explain accretion rates next to flooding regime variables.

The single negative beta coefficient of inundation frequency can again be linked to collinearity. The correlation between inundation frequency and accretion rate in the simple linear regression is positive on this location, meaning the negative beta coefficient must be due to collinearity on this particular location between cross-shore wind speed and inundation frequency.

Schiermonnikoog: R^2 and β -values of MLR models by SEB location

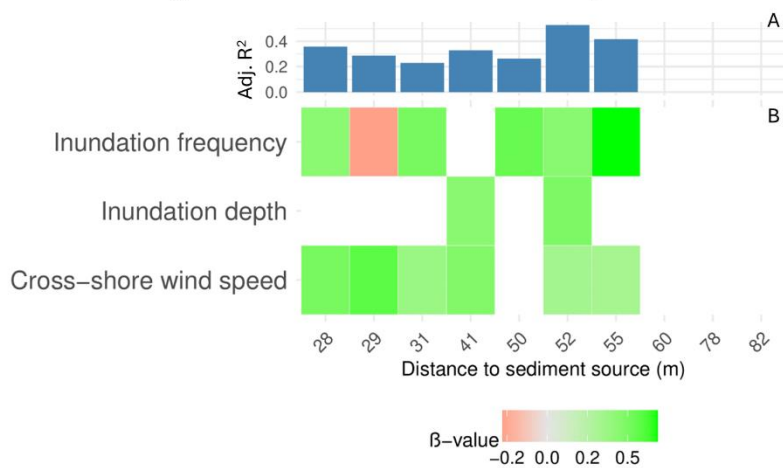


Figure 14:(A) Adjusted R^2 of significant MLR models for each SEB station plotted over distance to sediment source. (B) β -coefficients of explanatory variables in MLR models.

Spatial analysis

First the general spatial variability of accretion is presented in figures 15 and 16 for Ameland and Schiermonnikoog respectively. On Ameland accretion rate is clearly dependent on surface height, distance to creek, distance to shoreline and distance to sediment source which is the closest between the shoreline and creek. Both distance to shoreline and distance to tidal creek are important drivers of spatial variability on Ameland. The distance to sediment source, essentially combining both factors, is the most important driver of spatial variability on Ameland. A different pattern is found on Schiermonnikoog where only distance to shoreline causes spatial variability within our dataset. However, the range of the distance to creek is much smaller than on Ameland, so the effect of the tidal creek should still be the same on Schiermonnikoog, but it is not represented by the spatial coverage of the SEBs on Schiermonnikoog.

Ameland: Accretion Rate vs Spatial Variables

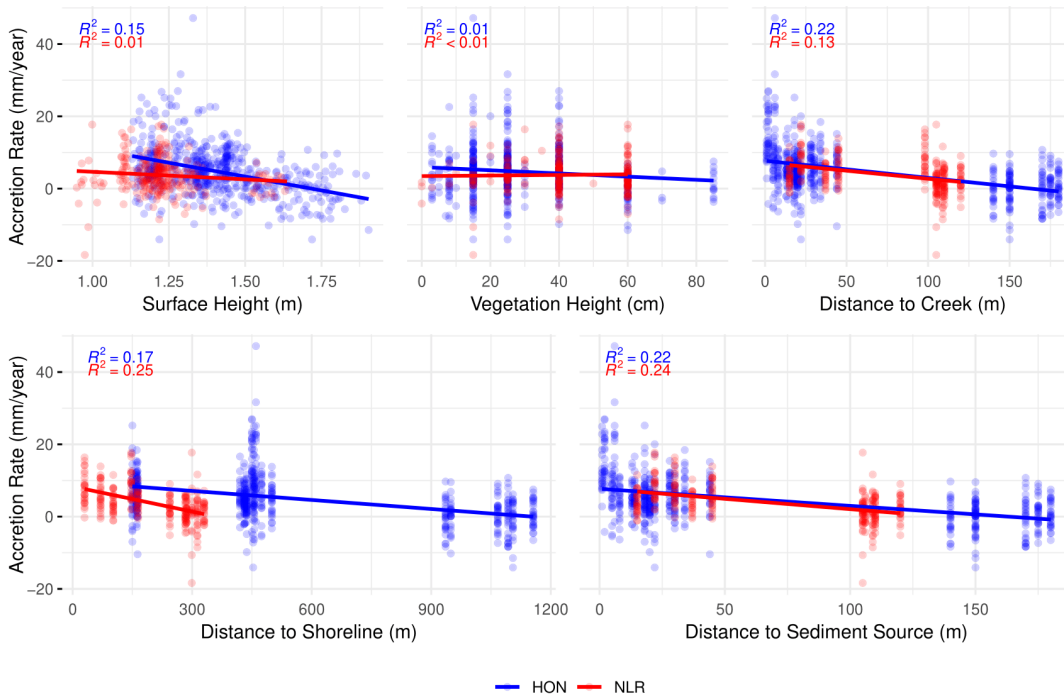


Figure 15: Relation between accretion rate and spatial variables on the two salt marshes on Ameland with R^2 of linear regression line.

Schiermonnikoog: Accretion Rate vs Spatial Variables

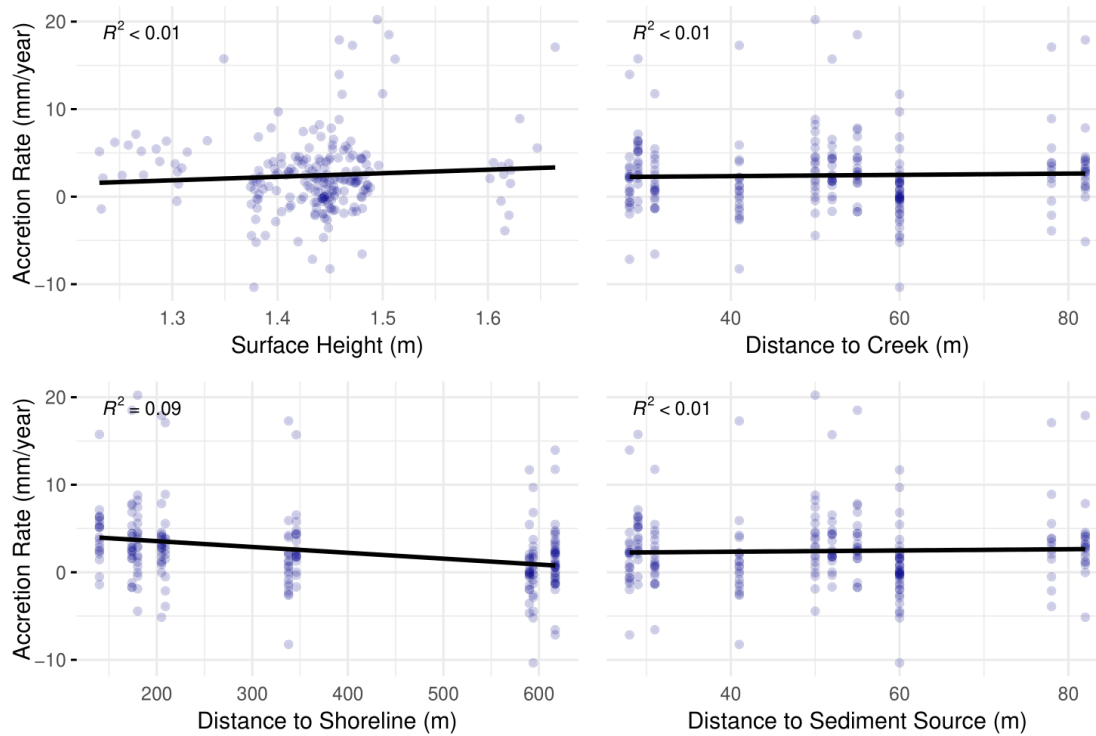
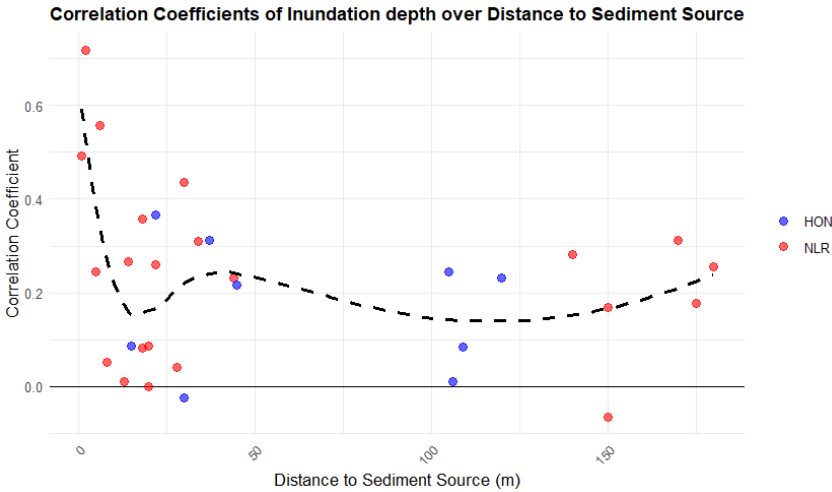


Figure 16: Relation between accretion rate and spatial variables on Schiermonnikoog salt marsh with R^2 of linear regression line.

The same correlation coefficients from the simple linear regression as presented in figures 8 and 9 are plotted as a function of the spatial variables (appendix 4). Two patterns were observed.

The first is the sharp decline of the correlation between inundation depth and accretion rate in the first meters moving away from the sediment source observed on Ameland (fig. 17). This pattern is only observed on Ameland, as Schiermonnikoog does not contain the same range in distance to sediment source. The pattern indicates that inundation depth has most influence on accretion rates on the part of the salt marsh within 25 meters from the sediment source.

The second pattern is the decline of the correlation between cross-shore wind speed and accretion rate over the distance to sediment source observed on Schiermonnikoog. This pattern is visible despite the smaller range of distance to sediment source on Schiermonnikoog. Therefore, it also suggests that the correlation of cross-shore wind speed to accretion rate would be higher in areas even closer to the sediment source.



Discussion

This study aims to evaluate how storm characteristics that influence SSC affect long-term marsh accretion rates, with a particular focus on identifying the drivers of spatial variability in storm-induced accretion. Using simple linear regression, individual relationships between storm variables and accretion rates were explored, followed by spatial analysis to assess variability across the marsh. MLR revealed that SSC-controlling variables added little explanatory power due to their collinearity with inundation depth. However, offshore wind emerged as a key storm characteristic associated with increased accretion. Furthermore, both inundation depth and cross-shore wind speed were found to be more influential in driving accretion near the shoreline and tidal creek areas. Building on these results, the following discussion contextualizes the findings and explores potential hydrodynamic processes driving the observed patterns.

Wave height

The wave height was expected to have an ambivalent effect on accretion. On one hand wave height contributes to accretion rates by increasing SSC through increasing wave orbital velocity and wave shear stress. On the other hand, local waves on the salt marsh during flooding can inhibit settling of suspended sediments or even cause local erosion.

In general, a weakly positive relation with accretion was found (fig. 8 & 9), which agrees with the expected effect. However, the observed effect of wave height on accretion proves to not be significant next to flooding regime variables in the MLR models (fig. 12 & 14).

Since the wave height is measured at the North Sea, 10 km north of Schiermonnikoog, the wave height represents fetch-unlimited conditions, which occur on the North Sea. Therefore, wave height is a proxy for SSC coming from the North Sea and to a lesser degree for SSC in the Wadden Sea through resuspension on less sheltered tidal flats. Mainly the latter is thought to be important since several studies found that the main source of SSC and salt marsh accretion is resuspension on tidal flats (Christiansen et al. 2006, Schuerch et al. 2014, Panozzo et al. 2023).

If SSC were the sole driver of salt marsh accretion, a strong positive relation between wave height and accretion would have been expected. However, depending on the wind direction, wave height of local waves on the salt marsh can be high. In this case the local waves prevent the suspended sediment from settling, which results in the observed weak correlation to wave height. This finding supports the importance of local wave conditions and dependency of accretion on fetch and wind direction.

Long-shore wind speed and absolute wind speed

The absolute wind speed and long-shore wind speed are highly correlated (figures 10 & 11). This makes sense as the long-shore wind speed roughly corresponds to a (south-)westerly wind direction, which is known to be the prevailing wind direction in the Dutch Wadden Sea (Gerkema et al. 2017). Due to the strong similarity between absolute wind speed and long-shore wind speed, their relationship with sediment accretion is also similar (figures 8 & 9). Therefore, for the remainder of this study, they will be treated as one.

It was expected that absolute wind speed would have a similar effect on accretion as the wave height, since wind speed determines wave height for a large part.

. Figures 8 and 9 reveal that the correlation between (long-shore) wind speed and accretion is generally weak, with both positive and negative correlations observed across different SEB locations. This is slightly different compared to the wave height.

The switching sign in the correlation suggests that local geomorphological conditions likely determine whether the effect of wind speed aligns with expectations, i.e., strong wind leading to high waves, inducing resuspension, increasing SSC, and resulting in higher accretion—or whether it leads to erosion instead. Since none of the spatial variables tested (Appendix 3) show a significant influence on the effect of long-shore wind speed on accretion, it is likely that the spatial variability in the effect of long-shore wind speed on accretion results from a combination of the tested spatial factors or from spatial variables that were not included in the analysis.

One possible explanation for the unexpected negative effects is that long-shore winds may contribute to erosion by generating waves within ponds in the marsh. The breaking of these waves over the pond edge could cause localized erosion (Mariotti et al. 2020).

Cross-shore wind speed

The cross-shore wind speed was expected to control SSC locally because of its effect on the fetch and wave height. The correlation between cross-shore wind speed and accretion is weak in the simple linear regression (fig. 8 & 9). However, when incorporated in the MLR model on Schiermonnikoog, together with the flooding regime variables, it becomes clear that cross-shore wind speed is significantly adding to the explanation of the variance in accretion rate.

Importantly, cross-shore wind speed shows no correlation with the flooding regime variables inundation depth and inundation frequency. This implies that cross-shore wind speed accounts for a process that is not contained by the flooding dynamics alone. However, the suggested mechanism of strong on-shore wind leading to locally high waves, resuspension and high SSC as found by Christiansen et al. 2006 and Duvall et al. 2019, is not at play here. This is because the cross-shore wind direction, in general, is in fact an offshore directed wind rather than the onshore wind, which is the direction associated with high SSC in literature.

However, the same literature also finds that due to the orientation of the studied salt marshes, the onshore wind direction, which causes high SSC, results in a set-down of the water level. This is the case in the Dutch Wadden Sea as well; a south-easterly wind (onshore) causes a set-down of the water level (Gerkema et al. 2017). As a result, the high SSC conditions caused by the onshore wind rarely occur during inundations of the salt marsh.

What could explain why offshore winds increase accretion rate is the following. Most storms in the study area have a strong westerly wind, which translates into a (slight) offshore wind at the salt marshes (Gerkema et al. 2017). These storms cause high SSC in the Wadden Sea in general. Although the local resuspension at the tidal flats will be lower, the SSC can still be high because of storm conditions elsewhere and advection of this high SSC during the storms.

The final mechanism that explains why the onshore winds capture a process that is not contained by the flooding variables is the settling of sediments in the water. Due to the offshore wind on the salt marsh, wave energy is low, meaning resuspension is low as well. Therefore, settling of the sediment is more efficient during offshore winds. This suggests that offshore-directed winds may contribute to accretion not through local resuspension necessarily, but through enhanced settling conditions and the delivery of suspended sediment from elsewhere in the Wadden Sea during storm events.

Storm surge height

Storm surge height shows a positive correlation to accretion rate, which is constant over space. On Ameland, the relation is rather weak but on Schiermonnikoog the relation is stronger. Storm surge height was expected to be a proxy for SSC, as storm surge is controlled by wind direction, wind speed, atmospheric pressure. Moreover, high storm surge increases tidal asymmetry, causing strong flood-flows which lead to current-induced resuspension of the tidal channels (Gerkema & Duran-Matute 2017). The observed positive relation seems to confirm this hypothesis.

However, the question is whether the storm surge height captures a different process than the inundation depth, since a higher storm surge height directly translates into a higher inundation depth. The collinearity with inundation depth is indeed relatively high (0.55), which indicates that the inundation depth captures partially the same effect as storm surge height. This is further confirmed by the MLR model in figure 12, which shows inflated beta coefficients for inundation depth and storm surge height due to the collinearity. Therefore, the storm surge height does not add to explanation of variance next to the flooding regime variables.

Inundation frequency and duration

Inundation frequency and duration were expected to contribute positively to accretion, as more frequent and prolonged inundation events provide increased opportunities for sediment deposition (Butzeck et al. 2015; Duvall et al. 2018). The observed relationship aligns with this expectation on Schiermonnikoog, where both inundation frequency and duration show a strong positive correlation with accretion rate (figures 8 & 9). In contrast, this relationship is weak on Ameland, suggesting site-specific factors may mediate the influence of inundation on accretion.

One possible explanation is the slight difference in average elevation of the SEBs. On Ameland the SEBs are located slightly lower than on Schiermonnikoog (10 cm on average), resulting in more frequent inundations on Ameland. Therefore, storm driven variability is diluted in the aggregated timeseries of inundation frequency on Ameland compared to Schiermonnikoog.

Vegetation is probably not a factor since vegetation is relatively similar on both islands. Based on vegetation observations by Bolding 2024, difference in vegetation between Hon and Schiermonnikoog is not expected to significantly alter sediment trapping efficiency.

Inundation frequency and total inundation duration are found to be highly correlated, which is logical: more frequent inundations naturally result in longer cumulative inundation times during the aggregation period. The only way for the two variables to not be collinear is if the average duration of inundations would differ between years. Since the two variables are correlated the average duration of one inundation must be the same each year. Their collinearity implies that the average duration per inundation remains relatively constant over time. So, it is not necessary to include both inundation frequency and duration as a storm variable.

Importantly, inundation frequency is largely independent of other storm-related variables, which reinforces its role as a key driver of accretion. This is supported by the multiple linear regression models, where inundation frequency frequently emerges as a significant explanatory variable. These findings are consistent with the conclusions of Schuerch et al. (2011) and Van Dobben et al. (2022), who also highlight the central role of inundation regime in governing long-term salt marsh accretion.

Inundation depth

Inundation depth mostly correlates positively to accretion rates which can be expected based on numerous studies that found inundation depth as one of the most important storm characteristics for storm-induced accretion (Schuerch et al. 2011; Tognin et al 2021). Collinearity between inundation depth and all SSC-controlling variables except cross-shore wind speed is observed. This indicates that (part of) the effect of SSC is contained by inundation depth.

In principle, it is already known that storms cause both a high water level and a high SSC, meaning that in general high inundation depths correspond to high SSC. However, as pointed out in the introduction, SSC can vary depending on wind direction and not every storm causes the same high-water levels as this depends on the interplay between astronomical tides, wind direction and wind speed (Needham & Keim 2014; Lyddon et al. 2018). Additionally, not every storm causes the same increase in SSC as this also depends on the tidal dynamics, wind conditions and on local geography (Christiansen et al. 2008; Ganju et al. 2013). This resulted in the idea that SSC dynamics and inundation depth were decoupled from each other. Consequently, it was hypothesized that with the introduction of the SSC-controlling variables next to the already researched flooding variables, accretion rates could be better explained. However, the correlation matrices indicate that the SSC-controlling variables are correlated to the inundation depth, which means that the inundation depth is a better proxy for SSC than was thought before based on the studies of Christiansen et al. (2006) and Ganju et al. (2013).

The most likely explanation for the result that SSC-controlling variables do not provide additional predictive power for accretion rates, although decoupling of SSC and inundation depth is observed in previous research, must lie in the yearly aggregation of the data that is used in this study as well as by Schuerch et al. (2011) and Van Dobben et al. (2022). The decoupling of SSC to inundation depth is observed on the much finer temporal scale of several days, covering individual storms and tidal cycles. However, when averaging over one year, the general trend of high SSC during more intense storms which cause higher water levels, prevails and the trends on small temporal scale are averaged out. What can be concluded is that the mean inundation depth over one year is a good indicator for storm driven SSC dynamics and storm intensity in general.

Spatial variability of storm-induced accretion

Spatial patterns are observed in the correlation between inundation depth and accretion rate on Ameland and between cross-shore wind speed and accretion rate on Schiermonnikoog. In both patterns the correlation decreases sharply over increasing distance to sediment source. This indicates that either accretion rates near the shoreline or tidal creek are more directly impacted by storm-induced accretion than locations further away from the shoreline or tidal creek or significant post-storm redistribution of sediment occurs on the interior marsh. Since the accretion measurements are yearly measurements, they reflect the net effect of all inundation events, including sediment redistribution. Therefore, it is most likely that accretion rates near the shoreline or tidal creek are more directly impacted by storm-induced accretion than accretion rates on the interior marsh.

It is known that accretion rates are higher close to sediment sources because once water flows over channel banks it drops out of suspension causing the locations close to tidal creeks to have higher accretion rates than the areas on the marsh that are further from the sediment source

(Temmerman et al. 2003). This process is also present in this study area as can be observed from the average accretion rates presented in figure 2B.

However, if we assume that minerogenic accretion is the only process behind the accretion observed by the SEBs, then the relative share of storm-induced accretion must be the same regardless of distance to sediment source, which means that the correlation between accretion and storm variables is also independent of distance to sediment source. That is why it must be concluded that other processes than only the minerogenic accretion are also affecting the accretion measured by the SEBs.

Since there is more minerogenic accretion near the tidal creeks or shoreline, it dominates the accretion rates in these areas. Further from the sediment source, minerogenic accretion rates are lower, allowing other processes to have a relatively greater influence. Firstly, the in-situ organic matter production and deposition is a process that can be responsible for this. The organic matter production and deposition is affected by elevation through inundation frequency. Salt marsh species often have an optimal inundation frequency for growth (Morris et al. 2002). Therefore, the organic matter fraction typically increases with distance from the sediment source until a certain point as the salt marsh elevation increases with distance from the sediment source. So, the relative contribution of organic matter production and deposition can be responsible for a bigger share of the accretion further from the sediment source.

Secondly, the swelling and shrinking effect, which is known to affect the SEB measurements (Van Dobben et al. 2022) can be responsible as well for the decreasing storm effect further from the sediment source. Swelling and shrinking is a process that occurs on drying and rewetting of clays. The clay content on the salt marsh can increase with distance to sediment source, as the area close to the sediment source is inundated the first and the particles with a coarser grain size fall out of suspension first, leading to a gradient of clay content. This would suggest that salt marsh areas further from the sediment source are more affected by swelling and shrinking compared to areas close to the sediment source. This supports the idea that accretion measured by SEBs in these locations is influenced more by soil expansion/contraction and organic accumulation than by minerogenic inputs.

Consequently, storm-driven accretion is more clearly expressed near sediment sources, where minerogenic deposition dominates, while in more distal areas, SEB measurements reflect a greater influence of non-storm-related processes.

Difference between Ameland and Schiermonnikoog

In general, the variance in accretion rates is better explained by storm-related variables on Schiermonnikoog than on Ameland. This is evidenced by stronger simple linear regression correlations and higher R^2 values in the MLR models for Schiermonnikoog. These results suggest that storm characteristics play a more pronounced role in driving accretion on Schiermonnikoog compared to Ameland.

Notably, this discrepancy is not due to differences in average accretion rates. Figure 2B and 2C show that average accretion is similar between the two islands, and in fact, Ameland even shows higher values in some locations. However, these high-accretion sites on Ameland are situated very close to tidal creeks, which are not sampled by SEBs on Schiermonnikoog. As a result, the relative error introduced by the SEB measurements should be similar or higher on Schiermonnikoog. Therefore, differences in average accretion rate itself cannot explain the stronger correlation between storm events and accretion observed on Schiermonnikoog.

One possible explanation lies in the difference in clay thickness between the islands. According to Van Dobben et al. (2022), clay layers are thicker on Ameland (averaging 50 cm at NLR and 15 cm at HON) than on Schiermonnikoog (approximately 10 cm). Since swelling and shrinking due to moisture fluctuations are more pronounced in thicker clay layers, this process likely has a larger influence on SEB measurements on Ameland. Consequently, this could reduce the strength of correlations between storm variables and accretion, as a greater portion of measured surface elevation change on Ameland may result from physical soil dynamics rather than minerogenic sediment deposition.

However, the explanatory power of clay thickness alone appears insufficient. The clay thickness at HON on Ameland is relatively similar to that of Schiermonnikoog, yet the correlation between storm variables and accretion remains weak at HON, and MLR models do not exceed an R^2 of 0.2. In contrast, Schiermonnikoog achieves maximum R^2 values of up to 0.5. This suggests that while swelling and shrinking effects linked to clay content may obscure storm-related signals on Neerlands Reid, they do not account for the weaker relationships on Hon compared to Schiermonnikoog.

Another key difference lies in the role of soil subsidence. Ameland has experienced anthropogenic subsidence due to gas extraction, with rates that were highest shortly after extraction began in 1984 and then decreased logarithmically over time (NAM 2023). Relative sea-level rise (RSLR), whether natural or human-induced, is generally associated with increased accretion rates as salt marshes adjust to maintain elevation (Hofsted et al. 2018). However, there is typically a time lag between RSLR and a corresponding rise in accretion, due to the marsh's delayed response in sediment accumulation (Hofstede et al. 2018). Thus, some of the variability in accretion on Ameland may be driven by subsidence-related RSLR rather than storm dynamics, thereby weakening correlations with storm variables. Additionally, if marshes on Ameland are still adjusting to past peaks in subsidence, this temporal lag could mask storm-related signals in the accretion data. The fact that the Hon has been subject to more subsidence than Neerlands Reid (fig. 2A), would make this effect more pronounced on the Hon.

In conclusion, the observed stronger correlation between storm characteristics and accretion on Schiermonnikoog may be influenced by factors such as clay thickness reducing the influence of swelling and shrinking, and subsidence, which allows storm dynamics to emerge more clearly in the accretion signal. While these mechanisms are plausible based on previous studies and known site conditions, they have not been directly quantified or tested in the current analysis. Therefore, their role should be explored further in future work.

Future Research Recommendations

This study aimed to explore the mechanisms through which storms influence accretion. The approach of aggregating storm-related variables has provided valuable insights such as the role of cross-shore winds for accretion next to flooding regime. Future research should build on this by examining storm characteristics at the level of individual events. High temporal resolution data on accretion, SSC, and storm dynamics, would enable better understanding of the processes at play during specific storm events. Part of this data could be obtained from Van Prooijen et al. 2020 for turbidity and from Adema et al. 2008 for storm dynamics. Such studies could reveal which storm parameters are most influential and how different types of storms mobilize sediments from various sources, such as the fringing intertidal flat, the broader tidal basin, the Wadden Sea, or even the North Sea. This would further support the direct prediction of how changes in storm regimes might affect accretion rates.

Reducing the number of explanatory variables by combining them into bulk parameters could further improve the predictive value of accretion models. An example of a bulk parameter could be (wave-induced) bed shear stress. This can be calculated for every timestep using equations 1-3. The additional data required is wave height and period measurements in the Wadden Sea with known bed elevation to calculate the water depth. Aggregation would still be necessary, but the advantage of this method is that the non-linear functions (eq. 1-3) combine water depth, wave period and wave height through physically meaningful formulas. This makes bed shear stress a more physically representative and informative variable to relate to accretion rate compared to the linear regression using different storm characteristics as explanatory variables as is done in this study.

Combining realistic wave dynamics and the idea of bulk parameters can be done in calculating the bed shear stress using equations 1-3. For every timestep the bed shear stress can be calculated. Aggregation would still be necessary, but the advantage of this method is that the non-linear functions (eq. 1-3) are applied in the bed shear stress parameter, making the bed shear stress a more physically representative and informative variable to relate to accretion rate compared to the linear regression using different storm characteristics as explanatory variables as is done in this study.

Another major improvement would be to model wave propagation towards and across the salt marsh. Waves play a critical role in sediment suspension and transport, yet in this study only wave-related variables near the measurement station were used. A spatially explicit simulation of wave energy could provide a much clearer understanding of where and how sediment is delivered to different parts of the marsh. The SWAN-model (Simulating Waves Nearshore) is a well-established numerical model for simulating the propagation and dissipation of waves in shallow coastal environments. The work of Christie et al. 2018 for example successfully adapted and applied the SWAN-model to British salt marshes. Implementing a similar model in this context would create the opportunity to study the effect of storm winds on accretion in greater detail.

Another promising direction is the use of hydrodynamic and sediment transport models to simulate the physical processes that influence storm-driven accretion in more detail. Specifically, the hydrodynamic model created by Duvall et al. 2019, which simulates coupled SSC and sediment flux next to hydrodynamics in 1D, can be calibrated and validated in this setting. This would allow for event-scale validation of the hypotheses presented in this study, such as the role of cross-shore wind and inundation depth, under realistic hydrodynamic conditions. In addition, Delft3D-FLOW, optionally coupled with sediment transport modules, can be used to simulate the spatial distribution of currents and sediment deposition across the marsh surface. This was successfully done by Willemsen et al. 2022 and Temmerman et al. 2005. Further coupling with SWAN can be used to model how wave energy dissipates spatially from the tidal flat onto the marsh under storm conditions. Using these models, parameters such as bed shear stress, sediment flux, and SSC can be calculated per timestep to analyse the effect of storm characteristics on SSC and accretion.

For larger scale sediment transport the tidal-basin scale hydrodynamic and sediment transport model by Sassi et al. (2015) can be useful. It provides valuable insights into the net movement of sediment through multiple tidal inlets in the Dutch Wadden Sea. While this model does not resolve marsh-scale processes, it could help identify sediment sources and dominant pathways during and after storm events. Such information would complement the finer-scale models

mentioned before by improving boundary conditions or finding where storm-mobilized sediments are likely coming from and on what storm characteristics this depends.

Finally, the role of soil moisture in driving swelling and shrinking processes is currently unclear. Although SEB measurements are known to be affected by these physical processes, there is a lack of comprehensive studies specifically examining the influence of soil moisture variability on SEB measurements in clay-dominated salt marshes. Understanding this relationship is crucial for improving the interpretation of SEB-derived accretion data.

Conclusion

This study investigated how storms influence sediment accretion on salt marshes by correlating yearly accretion rates to aggregated storm characteristics. The primary aim was to assess whether SSC-controlling variables offer additional explanatory power beyond the established flooding regime variables, which are inundation depth and inundation frequency.

The results show that SSC-controlling variables do not significantly improve predictions of long-term accretion when added to models including inundation depth and frequency. This is likely because inundation depth indirectly captures much of the SSC signal at annual timescales, making it a more powerful predictor of accretion than previously recognized.

One exception is cross-shore wind speed, which significantly contributes to explaining accretion variability. The proposed mechanism is twofold: offshore winds can elevate SSC through resuspension while simultaneously creating low wave conditions on the marsh that promote sediment settling. These conditions can amplify both sediment availability and deposition potential, leading to increased accretion during such events.

Spatially, the influence of inundation depth and cross-shore wind speed declines with increasing distance from sediment sources such as tidal creeks and shorelines. This suggests that storm-driven accretion is most pronounced near these sediment sources. In contrast, areas farther inland appear to be more influenced by other processes, including in-situ organic production and the effects of soil swelling and shrinking.

In summary, storms are key drivers of accretion on both islands, more so on Schiermonnikoog than on Ameland, which may relate to subsidence compensating accretion on Ameland. While SSC dynamics are important on the timescale of single flood events, their influence is effectively represented by inundation depth on the yearly timescale. Cross-shore wind speed emerges as a distinct and relevant factor. Crucially, the diminishing storm effect with distance from sediment sources underscores the importance of spatial context in evaluating marsh resilience. These insights are vital for predicting salt marsh adaptation under future climate and storm regime changes.

References

- Ahmad, A. U., Balakarishnan, U. v., & Jah, P. S. (2019). Detection of collinearity effects on explanatory variables and error terms in multiple regressions. *International Journal of Innovative Technology and Exploring Engineering*, 8(6 Special Issue 4), 1584–1591. <https://doi.org/10.35940/ijitee.F1319.0486S419>
- Andrée, E., Drews, M., Su, J., Larsen, M. A. D., Drønen, N., & Madsen, K. S. (2022). Simulating wind-driven extreme sea levels: Sensitivity to wind speed and direction. *Weather and Climate Extremes*, 36. <https://doi.org/10.1016/j.wace.2022.100422>
- Baaij, B. M., Kooijman, J., Limpens, J., Marijnissen, R. J. C., & van Loon-Steensma, J. M. (n.d.). *Monitoring Impact of Salt-Marsh Vegetation Characteristics on Sedimentation: an Outlook for Nature-Based Flood Protection*. <https://doi.org/10.1007/s13157-021-01467-w>/Published
- Barbier, E. B., Hacker, S. D., Kennedy, C., Koch, E. W., Stier, A. C., & Silliman, B. R. (2011). The value of estuarine and coastal ecosystem services. *Ecological Monographs*, 81(2), 169–193. <https://doi.org/10.1890/10-1510.1>
- Bartholomä, A., Kubicki, A., Badewien, T. H., & Flemming, B. W. (2009). Suspended sediment transport in the German Wadden Sea-seasonal variations and extreme events. *Ocean Dynamics*, 59(2), 213–225. <https://doi.org/10.1007/s10236-009-0193-6>
- Bolding, M. (2024). higher tides, lower marshes: how vegetation development on salt marshes is influenced by elevation. [unpublished master's thesis]. Wageningen University
- Butzeck, C., Eschenbach, A., Gröngroft, A., Hansen, K., Nolte, S., & Jensen, K. (2015). Sediment Deposition and Accretion Rates in Tidal Marshes Are Highly Variable Along Estuarine Salinity and Flooding Gradients. *Estuaries and Coasts*, 38(2), 434–450. <https://doi.org/10.1007/s12237-014-9848-8>
- Castillo, J. M., Gallego-Tévar, B., Castellanos, E. M., Figueroa, M. E., & Davy, A. J. (2021). Primary succession in an Atlantic salt marsh: From intertidal flats to mid-marsh platform in 35 years. *Journal of Ecology*, 109(8), 2909–2921. <https://doi.org/10.1111/1365-2745.13692>
- Cazenave, A., & Cozannet, G. le. (2014). Sea level rise and its coastal impacts. *Earth's Future*, 2(2), 15–34. <https://doi.org/10.1002/2013ef000188>
- Christiansen, C., Vølund, G., Lund-Hansen, L. C., & Bartholdy, J. (2006). Wind influence on tidal flat sediment dynamics: Field investigations in the Ho Bugt, Danish Wadden Sea. *Marine Geology*, 235(1-4 SPEC. ISS.), 75–86. <https://doi.org/10.1016/j.margeo.2006.10.006>
- Christie, E. K., Möller, I., Spencer, T., & Yates, M. (2018). modelling wave attenuation due to salt marsh vegetation using a modified swan model. *Coastal Engineering Proceedings*, 36. <https://doi.org/https://doi.org/10.9753/icce.v36.papers.73>
- Cornacchia, L., van de Vijssel, R. C., van der Wal, D., Ysebaert, T., Sun, J., van Prooijen, B., de Vet, P. L. M., Liu, Q. X., & van de Koppel, J. (2024). Vegetation traits and biogeomorphic complexity shape the resilience of salt marshes to sea-level rise. *Communications Earth and Environment*, 5(1). <https://doi.org/10.1038/s43247-024-01829-2>

- Cortese, L., Zhang, X., Simard, M., & Fagherazzi, S. (2024). Storm Impacts on Mineral Mass Accumulation Rates of Coastal Marshes. *Journal of Geophysical Research: Earth Surface*, 129(3). <https://doi.org/10.1029/2023JF007065>
- Couvillion, B. R., Steyer, G. D., Wang, H., Beck, H. J., & Rybczyk, J. M. (2013). Forecasting the effects of coastal protection and restoration projects on wetland morphology in coastal Louisiana under multiple environmental uncertainty scenarios. *Journal of Coastal Research*, 67(SPEC. ISSUE), 29–50. https://doi.org/10.2112/SI_67_3
- de Groot, A. v., Veeneklaas, R. M., & Bakker, J. P. (2011). Sand in the salt marsh: Contribution of high-energy conditions to salt-marsh accretion. *Marine Geology*, 282(3–4), 240–254. <https://doi.org/10.1016/j.margeo.2011.03.002>
- de Vlas, J. (2017). *Samenvatting Monitoring effecten van bodemdaling op Ameland-Oost: evaluatie na 30 jaar gaswinning*.
- Dijkema, K., van Dobben, H., Koppenaar, E., Dijkman, E., & van Duin, W. (2011). *Kweldervegetatie Ameland 1986-2010: effecten van bodemdaling en opslibbing op Neerlands Reid en De Hon*. <https://www.waddenzee.nl/thema/diepe-delfstoffen/bodemdaling-ameland/rapportage-2011/>
- Drexler, J. Z., Woo, I., Fuller, C. C., & Nakai, G. (2019). Carbon accumulation and vertical accretion in a restored versus historic salt marsh in southern Puget Sound, Washington, United States. *Restoration Ecology*, 27(5), 1117–1127. <https://doi.org/10.1111/rec.12941>
- Duvall, M. S., Wiberg, P. L., & Kirwan, M. L. (2019). Controls on Sediment Suspension, Flux, and Marsh Deposition near a Bay-Marsh Boundary. *Estuaries and Coasts*, 42(2), 403–424. <https://doi.org/10.1007/s12237-018-0478-4>
- Elschot, K., Baptist, M. J., & van Puijenbroek, M. E. B. (2023). Biocompacting livestock accelerate drowning of tidal salt marshes with sea level rise. *Frontiers in Marine Science*, 10. <https://doi.org/10.3389/fmars.2023.1129811>
- Elschot, K., de Groot, A., Dijkema, K., Sonneveld, C., van der Wal, J., de Vries, P., & Brinkman, B. (2017). *4 Ontwikkeling kwelder Ameland-Oost*.
- Farrar, D. E., & Glauber, R. R. (1967). *Multicollinearity in Regression Analysis: The Problem Revisited* (Vol. 49, Issue 1). <https://about.jstor.org/terms>
- Ganju, N. K., Nidzieko, N. J., & Kirwan, M. L. (2013). Inferring tidal wetland stability from channel sediment fluxes: Observations and a conceptual model. *Journal of Geophysical Research: Earth Surface*, 118(4), 2045–2058. <https://doi.org/10.1002/jgrf.20143>
- Gerkema, T., & Duran-Matute, M. (2017). Interannual variability of mean sea level and its sensitivity to wind climate in an inter-tidal basin. *Earth System Dynamics*, 8(4), 1223–1235. <https://doi.org/10.5194/esd-8-1223-2017>
- Hofstede, J. L. A., Becherer, J., & Burchard, H. (2018). Are Wadden Sea tidal systems with a higher tidal range more resilient against sea level rise? *Journal of Coastal Conservation*, 22(1), 71–78. <https://doi.org/10.1007/s11852-016-0469-1>
- Kennish, M. J. (2001). Coastal Salt Marsh Systems in the U.S.: A Review of Anthropogenic Impacts. In *Source: Journal of Coastal Research* (Vol. 17, Issue 3). <https://www.jstor.org/stable/4300224>

- Kim, J. H. (2019). Multicollinearity and misleading statistical results. *Korean Journal of Anesthesiology*, 72(6), 558–569. <https://doi.org/10.4097/kja.19087>
- Leonardi, N., Carnacina, I., Donatelli, C., Ganju, N. K., Plater, A. J., Schuerch, M., & Temmerman, S. (2018). Dynamic interactions between coastal storms and salt marshes: A review. In *Geomorphology* (Vol. 301, pp. 92–107). Elsevier B.V. <https://doi.org/10.1016/j.geomorph.2017.11.001>
- Lyddon, C., Brown, J. M., Leonardi, N., & Plater, A. J. (2018). Uncertainty in estuarine extreme water level predictions due to surge-tide interaction. *PLoS ONE*, 13(10). <https://doi.org/10.1371/journal.pone.0206200>
- Mariotti, G., Spivak, A. C., Luk, S. Y., Ceccherini, G., Tyrrell, M., & Gonneea, M. E. (2020). Modeling the spatial dynamics of marsh ponds in New England salt marshes. *Geomorphology*, 365. <https://doi.org/10.1016/j.geomorph.2020.107262>
- Mcdonald, R. P. (1989). An Index of Goodness-of-Fit Based on Noncentrality. *Journal of Classification*, 6, 97–103. <https://doi.org/https://doi.org/10.1007/BF01908590>
- NAM (2017). *Long Term Subsidence vervolgstudie*. <https://nam-onderzoeksrapporten.data-app.nl/reports/download/wadden/nl/e9129689-ebe7-4c29-ba92-a0f4ea434115>
- NAM (2023). *Gaswinning vanaf de locaties Moddergat, Lauwersoog en Vierhuizen*.
- Needham, H. F., & Keim, B. D. (2014). Correlating storm surge heights with tropical cyclone winds at and before landfall. *Earth Interactions*, 18(7), 1–26. <https://doi.org/10.1175/2013EI000527.1>
- Nolte, S., Koppenaar, E. C., Esselink, P., Dijkema, K. S., Schuerch, M., de Groot, A. v, Bakker, J. P., & Temmerman, S. (2013). Measuring sedimentation in tidal marshes: a review on methods and their applicability in biogeomorphological studies. In *Source: Journal of Coastal Conservation* (Vol. 17, Issue 3). <https://doi.org/https://doi.org/10.1007/s11852-013-0238-3>
- PannoZZo, N., Leonardi, N., Carnacina, I., & Smedley, R. K. (2023). Storm sediment contribution to salt marsh accretion and expansion. *Geomorphology*, 430. <https://doi.org/10.1016/j.geomorph.2023.108670>
- Patrick, L., Solecki, W., Jacob, K. H., Kunreuther, H., & Nordenson, G. (2015a). New York City panel on climate change 2015 report chapter 3: Static coastal flood mapping. *Annals of the New York Academy of Sciences*, 1336(1), 45–55. <https://doi.org/10.1111/nyas.12590>
- Patrick, L., Solecki, W., Jacob, K. H., Kunreuther, H., & Nordenson, G. (2015b). New York City panel on climate change 2015 report chapter 3: Static coastal flood mapping. *Annals of the New York Academy of Sciences*, 1336(1), 45–55. <https://doi.org/10.1111/nyas.12590>
- Sassi, M., Duran-Matute, M., van Kessel, T., & Gerkema, T. (2015). Variability of residual fluxes of suspended sediment in a multiple tidal-inlet system: the Dutch Wadden Sea. *Ocean Dynamics*, 65(9–10), 1321–1333. <https://doi.org/10.1007/s10236-015-0866-2>
- Schrijvershof, R. (2017). *Memo n.a.v. aandachtspunten rapport Analyse LiDAR data voor het Friesche Zeegat (2010-2016)*.

- Schuerch, M., Dolch, T., Reise, K., & Vafeidis, A. T. (2014). Unravelling interactions between salt marsh evolution and sedimentary processes in the Wadden Sea (southeastern North Sea). *Progress in Physical Geography*, 38(6), 691–715. <https://doi.org/10.1177/0309133314548746>
- Schuerch, M., Rapaglia, J., Liebetrau, V., Vafeidis, A., & Reise, K. (2012). Salt Marsh Accretion and Storm Tide Variation: An Example from a Barrier Island in the North Sea. *Estuaries and Coasts*, 35(2), 486–500. <https://doi.org/10.1007/s12237-011-9461-z>
- Schuerch, M., Spencer, T., & Evans, B. (2019). Coupling between tidal mudflats and salt marshes affects marsh morphology. *Marine Geology*, 412, 95–106. <https://doi.org/10.1016/j.margeo.2019.03.008>
- Soulsby, R. (1997). *Dynamics of Marine Sands: A Manual for Practical Applications*.
- Temmerman, S., Govers, G., Meire, P., & Wartel, S. (2003). Modelling long-term tidal marsh growth under changing tidal conditions and suspended sediment concentrations, Scheldt estuary, Belgium. *Marine Geology*, 193, 151–169. [https://doi.org/https://doi.org/10.1016/S0025-3227\(02\)00642-4](https://doi.org/https://doi.org/10.1016/S0025-3227(02)00642-4)
- Temmerman, S., Meire, P., Bouma, T. J., Herman, P. M. J., Ysebaert, T., & de Vriend, H. J. (2013). Ecosystem-based coastal defence in the face of global change. In *Nature* (Vol. 504, Issue 7478, pp. 79–83). <https://doi.org/10.1038/nature12859>
- Tognin, D., D'Alpaos, A., Marani, M., & Carniello, L. (2021). Marsh resilience to sea-level rise reduced by storm-surge barriers in the Venice Lagoon. *Nature Geoscience*, 14(12), 906–911. <https://doi.org/10.1038/s41561-021-00853-7>
- Tognin, D., D'Alpaos, A., Ghinassi, M., & Carniello, L. (2025). Marsh topography reveals the signature of storm-surge-driven sedimentation. *Geology*, 53(1), 45–49. <https://doi.org/10.1130/G52552.1>
- Turner, R. E., & Mo, Y. (2021). Salt marsh elevation limit determined after subsidence from hydrologic change and hydrocarbon extraction. *Remote Sensing*, 13(1), 1–14. <https://doi.org/10.3390/rs13010049>
- Turner, R. E., Swenson, E. M., & Milan, C. S. (2001). *organic and inorganic contributions to vertical accretion in salt marsh sediments*. Springer, Dordrecht. https://doi.org/https://doi.org/10.1007/0-306-47534-0_27
- van der Lugt, marlies, Visser, martijn, & ketelaar, G. (2020). *Monitoring wadplaatareaal Friesche Zeegat met LiDAR (2010-2019)*. <https://www.commissiemer.nl/projectdocumenten>
- van der Lugt Jelmer, M., Zheng, C., & Wang, B. (2020). *Integrale analyse morfologische effecten bodemdaling door gaswinning Ameland-Oost*. https://www.waddenzee.nl/publish/pages/17084/3-integrale_analyse_morfologie_ameland-oost_2024_.pdf
- van Dobben, H. F., de Groot, A. v., & Bakker, J. P. (2022). Salt Marsh Accretion With and Without Deep Soil Subsidence as a Proxy for Sea-Level Rise. *Estuaries and Coasts*, 45(6), 1562–1582. <https://doi.org/10.1007/s12237-021-01034-w>
- van Prooijen, B. C., Tissier, M. F. S., de Wit, F. P., Pearson, S. G., Brakenhoff, L. B., van Maarseveen, M. C. G., van der Vegt, M., Mol, J. W., Kok, F., Holzhauer, H., van der Werf, J. J., Vermaas, T., Gawehn, M., Grasmeijer, B., Elias, E. P. L., Tonnon, P. K., Santinelli, G., Antolínez, J.

A. A., de Vet, P. L. M., ... de Looff, H. (2020). Measurements of hydrodynamics, sediment, morphology and benthos on Ameland ebb-tidal delta and lower shoreface. *Earth System Science Data*, 12(4), 2775–2786. <https://doi.org/10.5194/essd-12-2775-2020>

van Puijenbroek, M., Sonneveld, C., & Elschot, K. (2024). *Ontwikkeling kwelders Oost-Ameland tijdens 35 jaar gaswinning*. <https://doi.org/10.18174/653049>

Willemsen, P. W. J. M., Smits, B. P., Borsje, B. W., Herman, P. M. J., Dijkstra, J. T., Bouma, T. J., & Hulscher, S. J. M. H. (2022). Modeling Decadal Salt Marsh Development: Variability of the Salt Marsh Edge Under Influence of Waves and Sediment Availability. *Water Resources Research*, 58(1). <https://doi.org/10.1029/2020WR028962>

Acknowledgements

I am deeply grateful to Roeland van de Vijssel, my first supervisor, for his continuous guidance with good spirits throughout this thesis journey. His thoughtful feedback and insightful additions consistently pushed my ideas further and helped shape this research. I also thank Ton Hoitink for his sharp critical perspective and for using his network to connect me with key researchers, which improved the depth of this work.

Special thanks go to Kelly Elschot for her support in data analysis and for offering fresh perspectives that helped me reinterpret my own findings. I am also thankful to Marinka van Puijenbroek, whose invitation to join fieldwork on the salt marshes of Ameland and Schiermonnikoog not only made this thesis possible but also brought in valuable ecological context that enhanced my understanding of the study area.

I greatly appreciate Nick Wallerstein for his role in setting up the laboratory experiments and for his creative, hands-on approach that was crucial in navigating experimental challenges. The lively and supportive environment in the HWM and SGL thesis rooms made all the difference thanks to my peers for both their helpful feedback and the good humour that kept things light during intense periods.

Finally, I am especially thankful to my friends and family for their support and encouragement. Their presence helped me stay grounded during the more difficult moments of this process.

Appendix 1: Cumulative aggregation method

The cumulative aggregation method refers to the method where all inundations events were summed for the aggregation period (one-year) to obtain aggregated timeseries for the explanatory variables. Here, a small analysis is shown in which the cumulative method is applied.

Figure 19 shows that intercorrelation is very high between the explanatory variables when using the cumulative approach. This is further supported by figures 20 and 21, which show that by using the cumulative approach, the explanatory variables become intercorrelated. This is not the case when using averaging (fig. 21).

For the simple linear regression the intercorrelation of the different storm variables is not important. Figure 22 shows the correlation coefficients between accretion and the storm variables when using the cumulative approach. When compared to figure 8, it becomes clear that using the cumulative approach does not result in better higher correlations.

Because in this study the goal is to find in which way and to what extent storm characteristics influence accretion, the averaging method was chosen to be able to see more differences between storm characteristics influence on accretion. This does not mean that the averaging method is perfect, because with averaging over one-year still a lot of potentially valuable information is lost. When compared to the cumulative aggregation method, the averaging method is the best option to be able to both include all inundation events in the analysis as well as compare the influence of different storm variables.

Ameland: Correlation Matrix for all explanatory variables

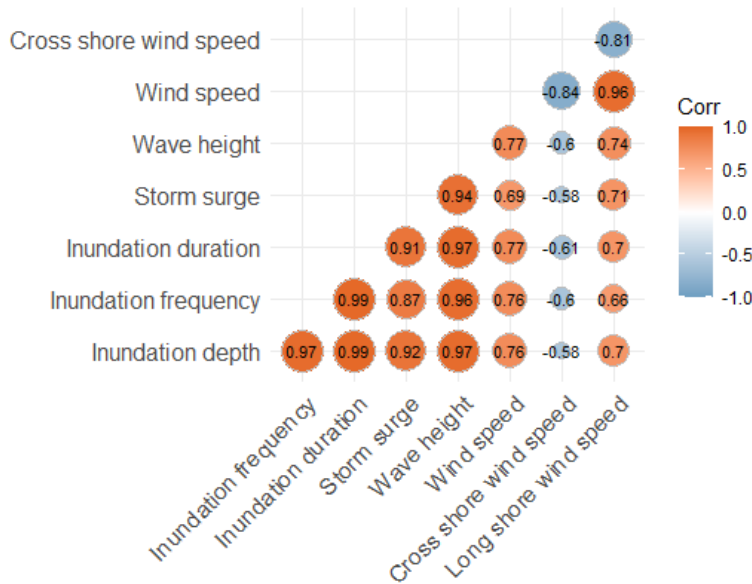


Figure 19: Correlation matrix using cumulative aggregation method on Ameland.

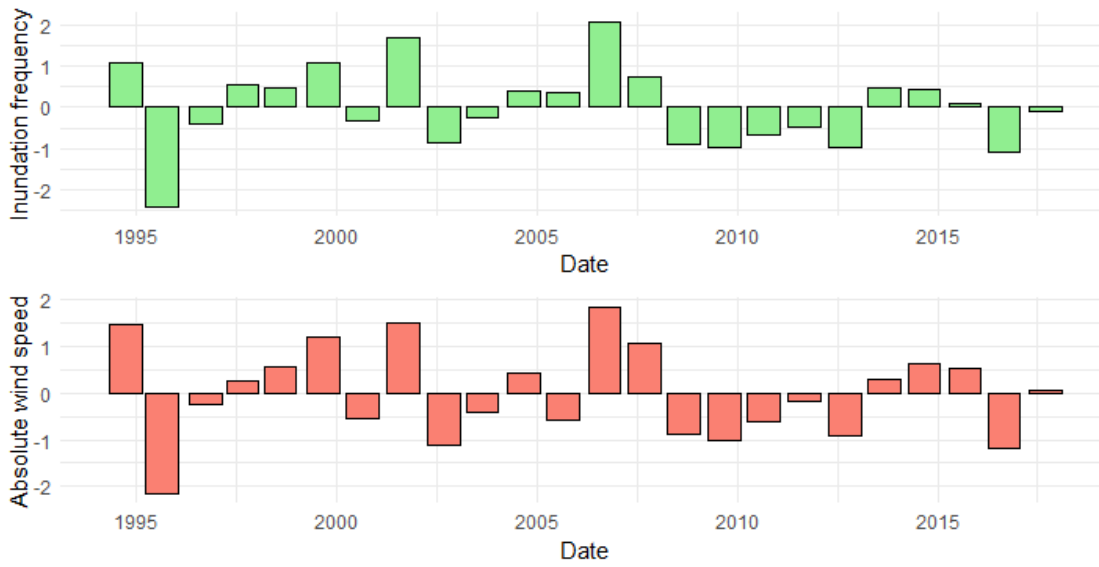


Figure 20: Aggregated timeseries of inundation frequency and absolute wind speed using the **cumulative** aggregation approach on one of the SEBs on Neerlands Reid. The y-axis is standardized, so the units are standard deviations.

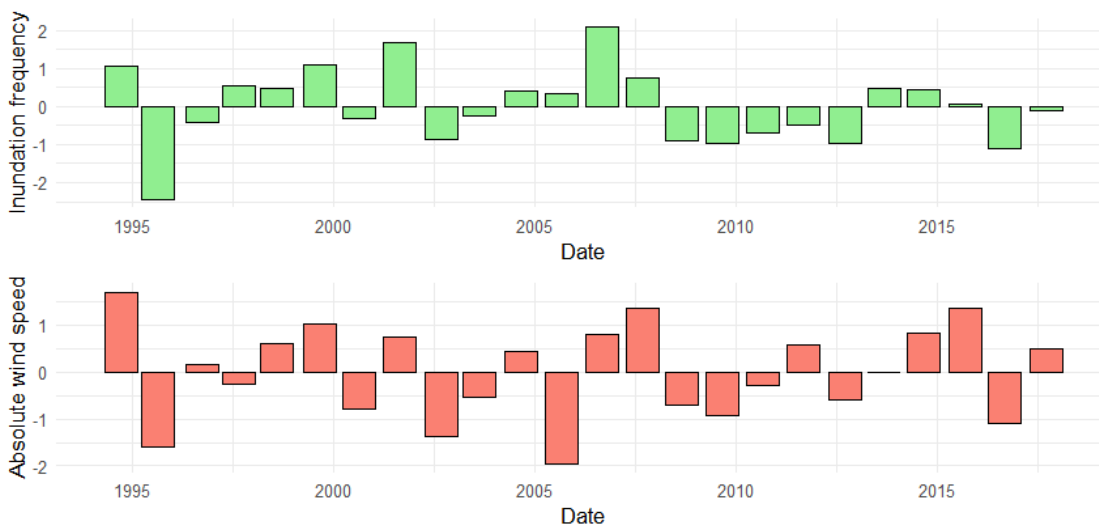


Figure 21: Aggregated timeseries of inundation frequency and absolute wind speed using the **averaging** aggregation approach on one of the SEBs on Neerlands Reid. The y-axis is standardized, so the units are standard deviations.

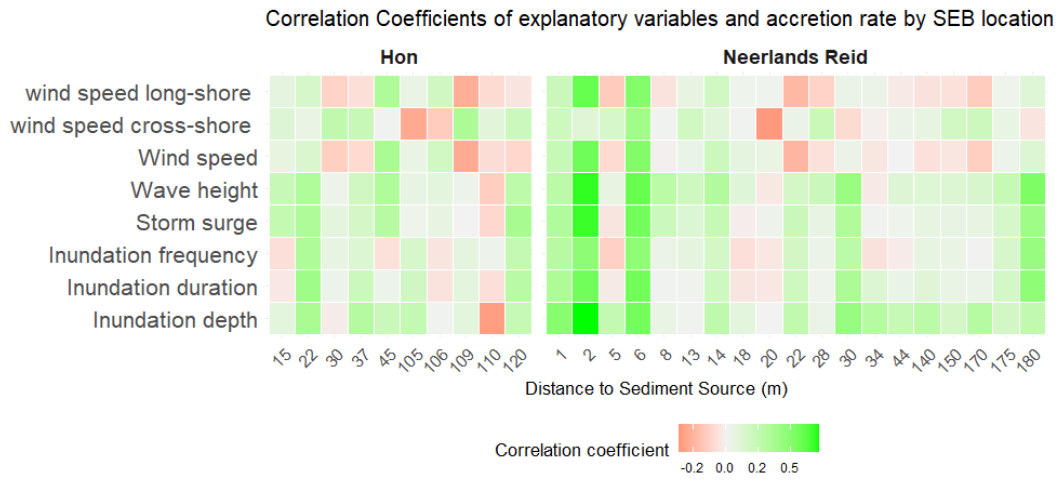


Figure 22: Pearson correlation coefficients of the simple linear regression between each explanatory variables and the accretion rate on each SEB on Ameland subdivided over the Hon and Neerlands Reid. The different SEB stations are represented on the x-axis by their distance to the sediment source. The cumulative approach was used for aggregation of the explanatory variables.

Appendix 2: Varying inundation depth threshold analysis

An attempt was made to replicate the threshold analysis by Schuerch et al. (2012), which found that inundation depth is the dominant accretion driver below 18 cm, while frequency dominates above 18 cm. Inundation depth and frequency are both put in a MLR model as explanatory variables with accretion rate as response variable. Next, flood events were filtered with increasingly high inundation threshold. For each inundation threshold, a new MLR was performed on the data of which the beta coefficients are plotted in the figures 23-25.

This pattern was not observed in our results (figures 23–25), likely due to differences in accretion measurement methods: SEBs used here may reflect shorter-term or non-accretion processes, unlike sediment cores. Importantly, increasing the inundation threshold did not improve the explanatory power of inundation variables (as shown by the R^2 in figures 23-25). This supports the approach used in the main analysis: considering all inundations is appropriate.

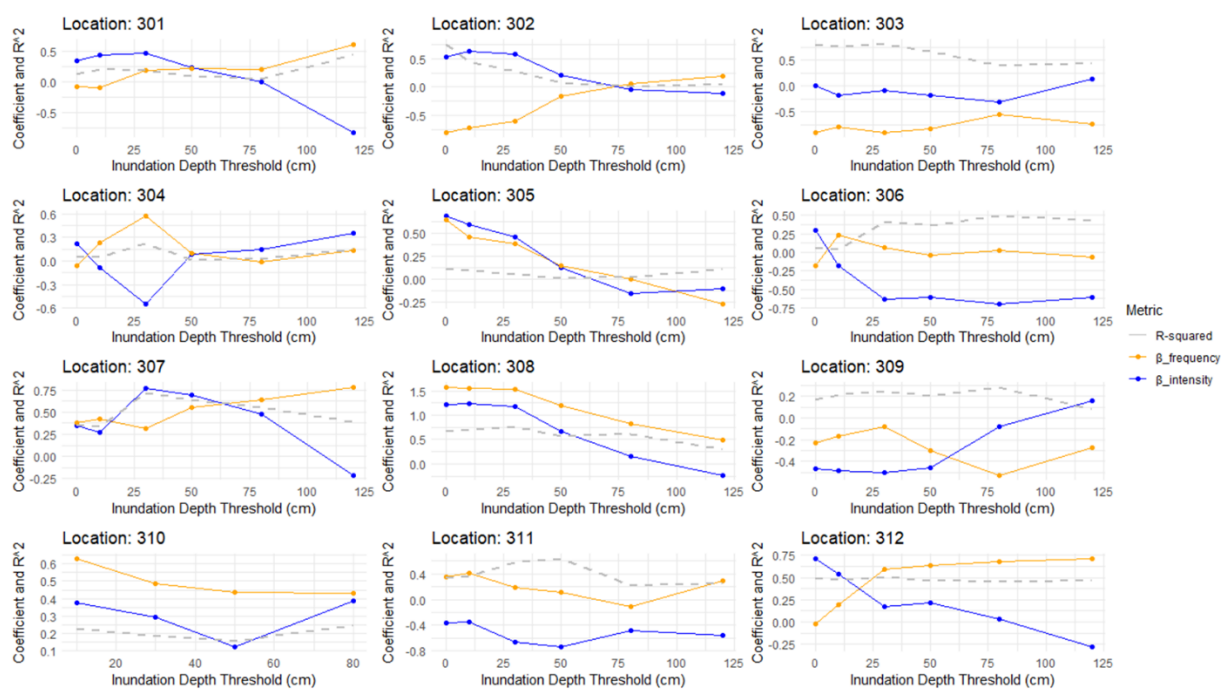


Figure 23: Analysis of varying inundation depth threshold for SEB locations 301-312. Blue and yellow are β -coefficients of inundation depth and inundation frequency respectively. Dotted line is the R^2 of the MLR model using inundation frequency and inundation depth as the only two explanatory variables.

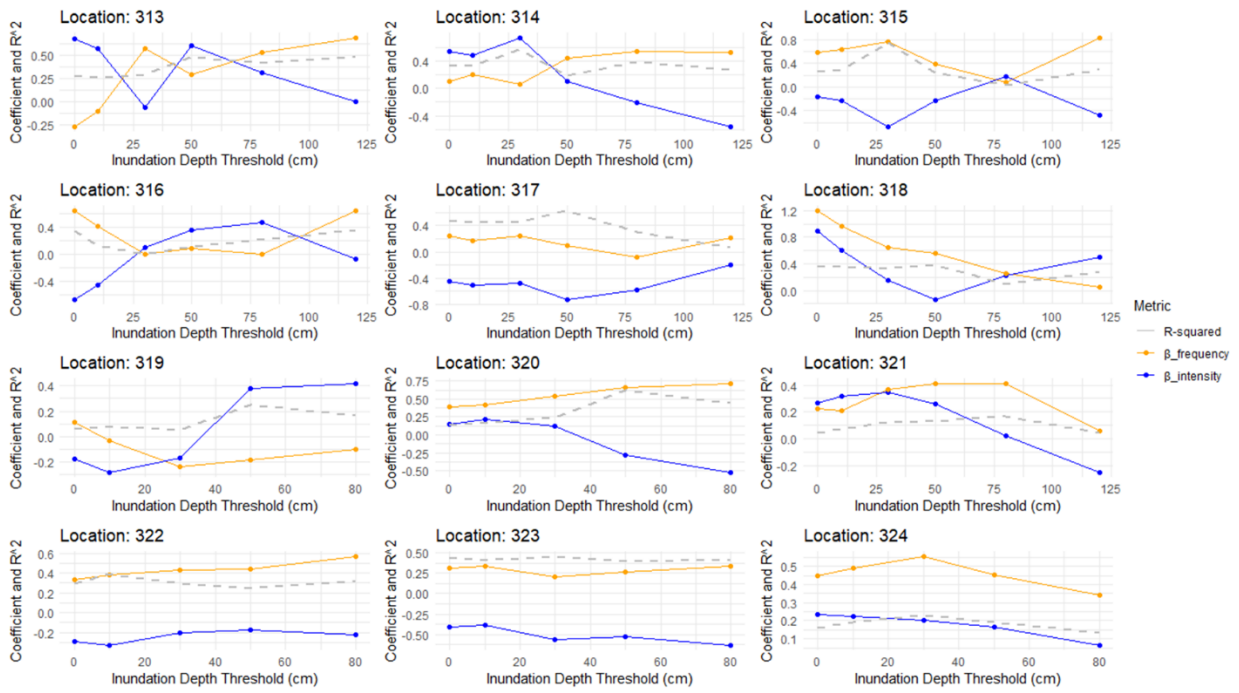


Figure 24: Analysis of varying inundation depth threshold for SEB locations 313-324. Blue and yellow are β -coefficients of inundation depth and inundation frequency respectively. Dotted line is the R^2 of the MLR model using inundation frequency and inundation depth as the only two explanatory variables.

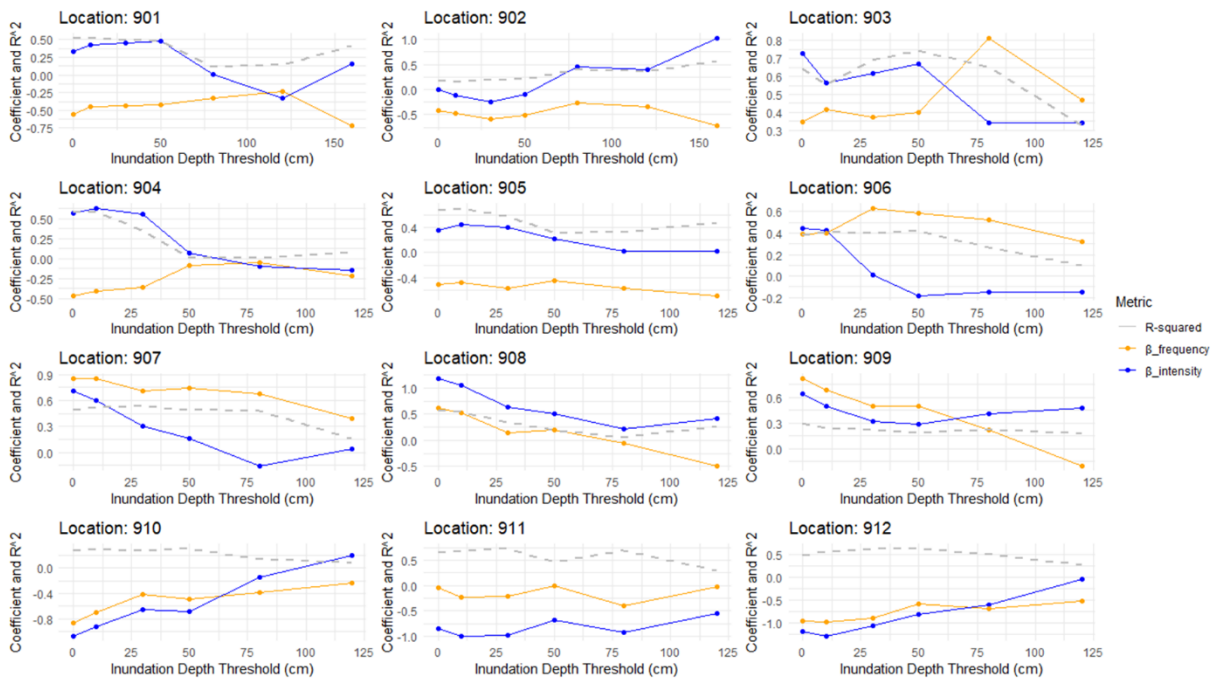


Figure 25: Analysis of varying inundation depth threshold for SEB locations on the Hon salt marsh (901-912). Blue and yellow are β -coefficients of inundation depth and inundation frequency respectively. Dotted line is the R^2 of the MLR model using inundation frequency and inundation depth as the only two explanatory variables.

Appendix 3: Analysis on period before inundation for SSC-variables

This appendix shows the analysis on which period before inundation should be used to determine the SSC-controlling variables. The tested periods range from 0 (conditions at peak inundation level) to 14 days. The tested periods are: 0, 0.5, 1, 2, 3, 7 and 14 days. Simple linear regression between accretion rate and SSC-controlling variables is performed using all periods. Equation 5 gives the general formula for simple linear regression in which ε is the residual.

$$y = \beta_0 + \beta_1 x + \varepsilon \quad (5)$$

The p-value of the beta coefficient (β_1 in equation 5) is plotted on the y-axis in figure 26-29. It is tested whether β_1 is significant with a student t-test, meaning that a smaller p-value indicates that the β_1 is more significant. In other words: the relation between SSC-controlling variable and accretion rate is more significant with smaller p-values.

While variability is high between SEB

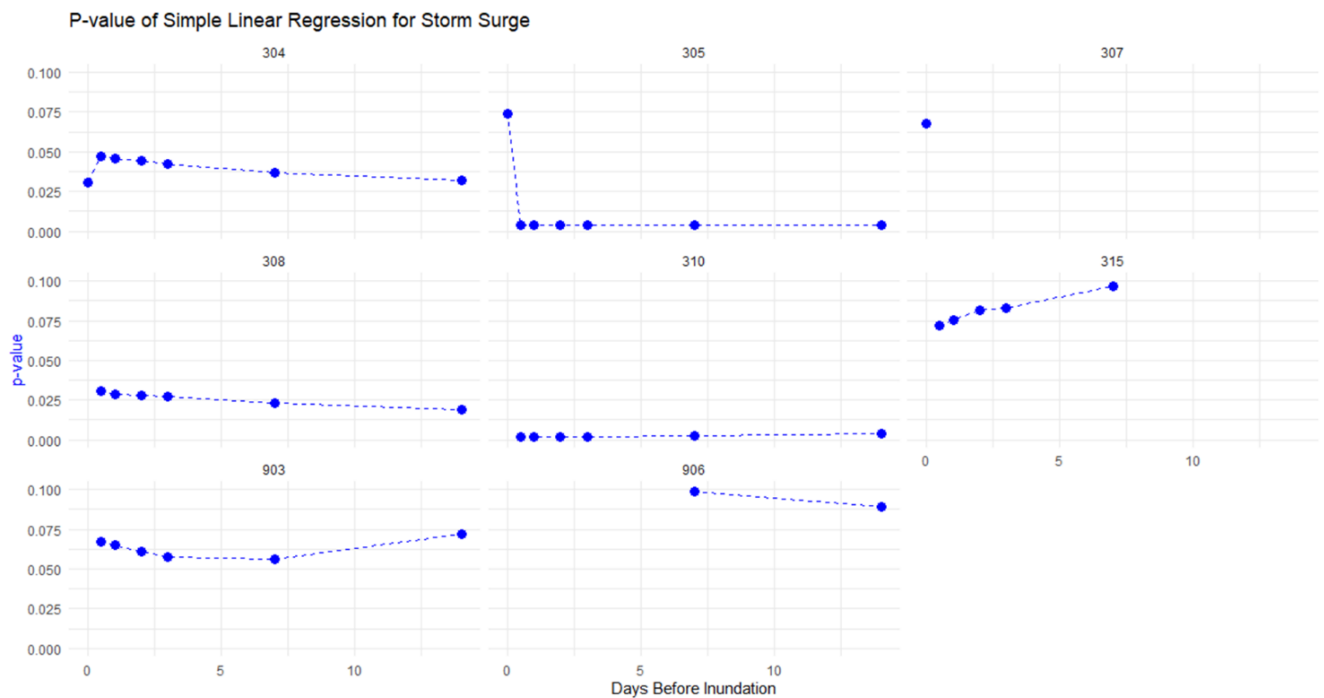


Figure 26: P-values of β_1 in Simple linear regression between storm surge and accretion rate with varying averaging periods before the start of the inundation. Different panels indicate different SEBs. Only the SEB locations with p-value smaller than 0.1 are shown.

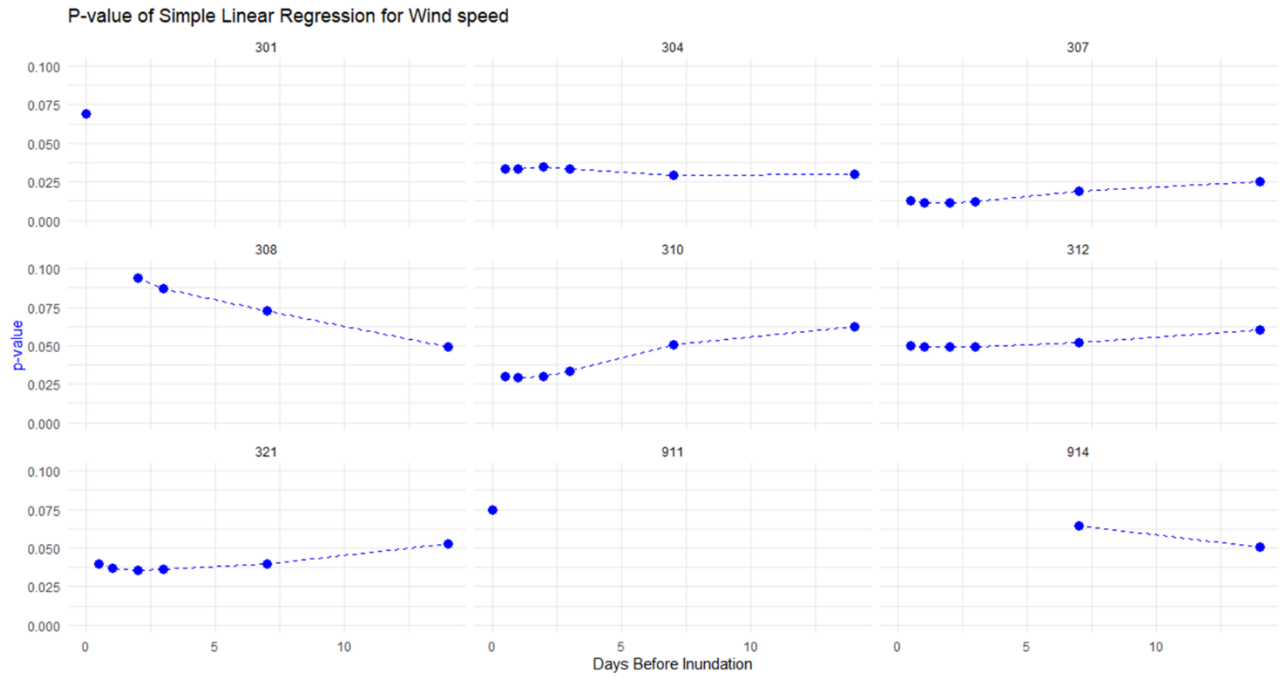


Figure 27: P-values of β_1 of simple linear regression between wind speed and accretion rate with varying averaging periods before the start of the inundation. Different panels indicate different SEBs. Only the SEB locations with p-value smaller than 0.1 are shown.

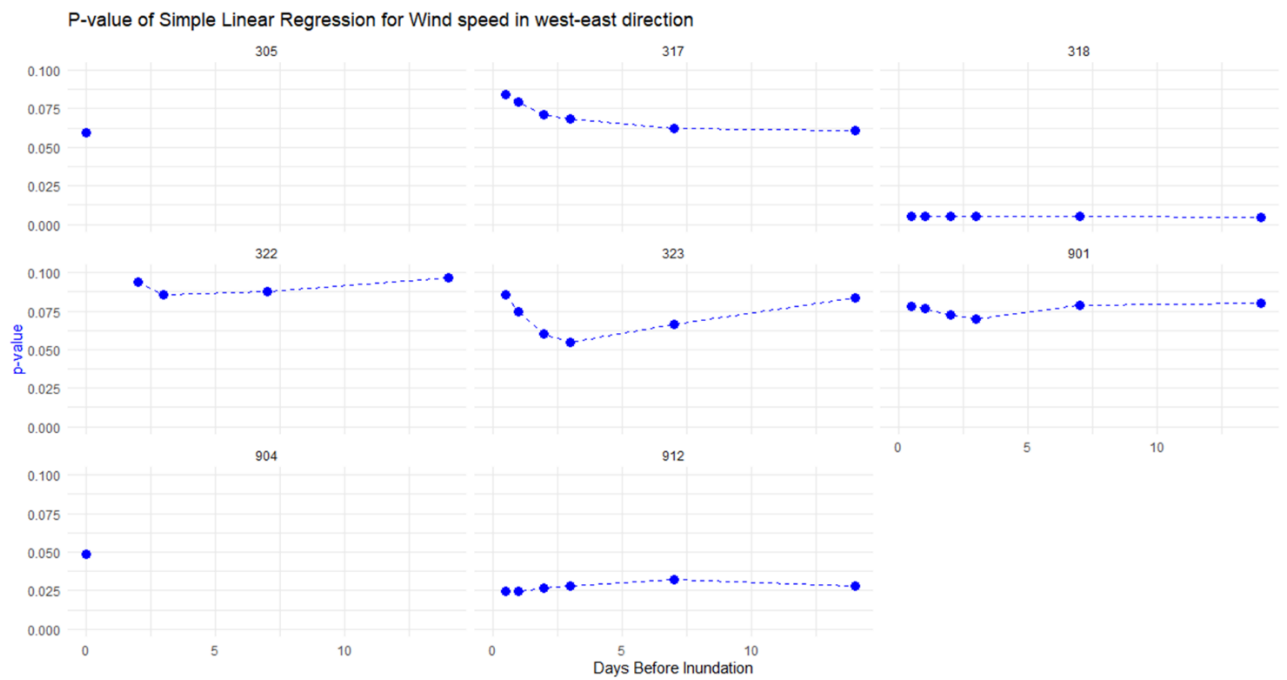


Figure 28: P-values of β_1 of simple linear regression between wind speed in west-east direction (roughly agreeing to long-shore direction) and accretion rate with varying averaging periods before the start of the inundation. Different panels indicate different SEBs. Only the SEB locations with p-value smaller than 0.1 are shown.

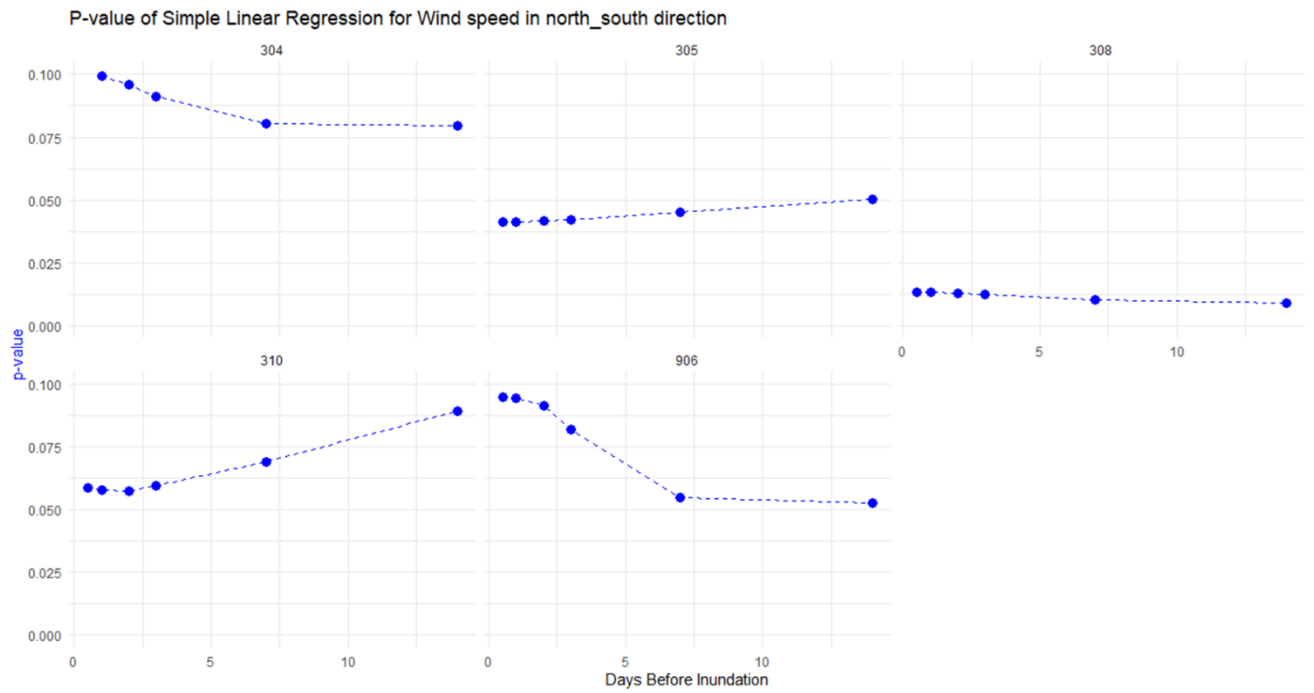


Figure 29: P-values of β_1 of simple linear regression between wind speed in north-south direction (roughly agreeing to cross-shore direction) and accretion rate with varying averaging periods before the start of the inundation. Different panels indicate different SEBs. Only the SEB locations with p-value smaller than 0.1 are shown.

Appendix 4: Analysis on drivers of intra-marsh variability of impact of storm characteristics on accretion rate

This appendix presents an analysis of how spatial marsh characteristics influence the relationship between accretion rates and storm-related explanatory variables. Correlation coefficients of accretion and storm variables are plotted over spatial variables in figures 30-38. The spatial variables included are:

- Distance to creek
- Distance to shoreline
- Distance to sediment source
- Surface elevation
- Vegetation height

Please note that for Schiermonnikoog, vegetation height was not included because this data was unavailable.

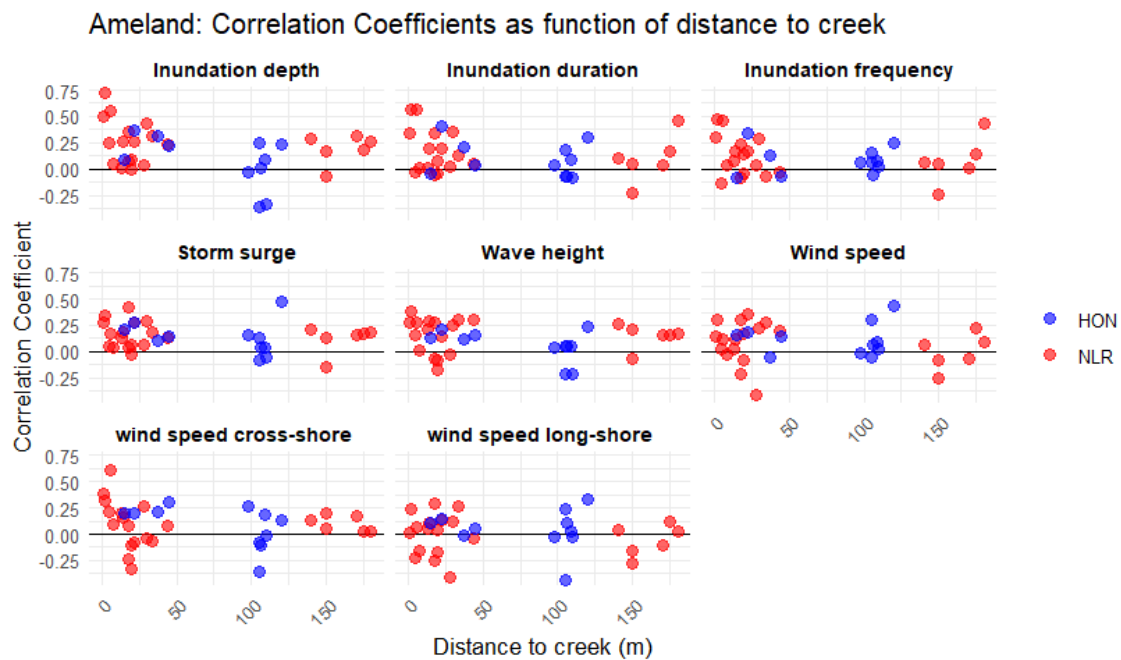


Figure 30: Correlation coefficients between accretion and storm variables on Ameland plotted as a function of distance to creek. Each panel has a different storm variable. The correlation coefficients are the same as presented in figure 8.

Ameland: Correlation Coefficients as function of distance to shoreline

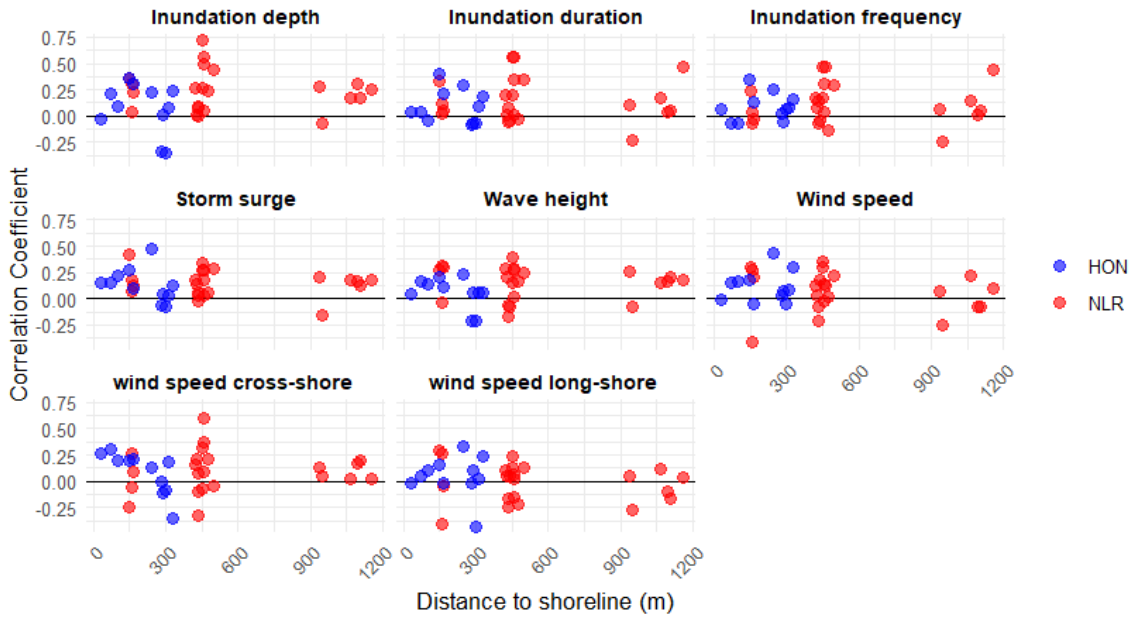


Figure 31: Correlation coefficients between accretion and storm variables on Ameland plotted as a function of distance to shoreline. Each panel has a different storm variable. The correlation coefficients are the same as presented in figure 8.

Ameland: Correlation Coefficients as function of distance to sediment source

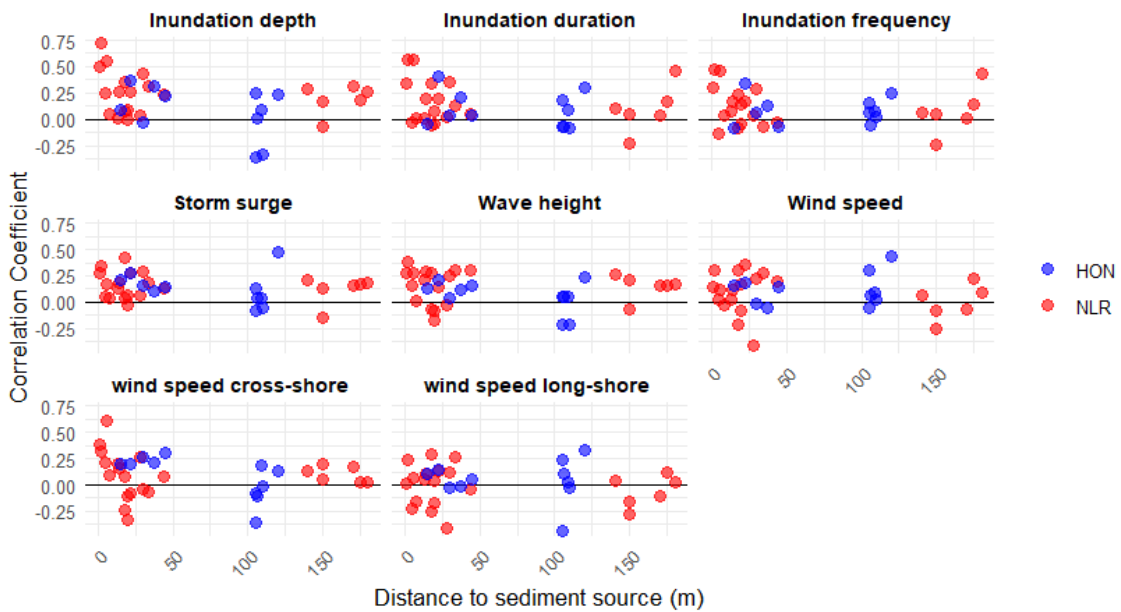


Figure 32: Correlation coefficients between accretion and storm variables on Ameland plotted as a function of distance to sediment source. Each panel has a different storm variable. The correlation coefficients are the same as presented in figure 8.

Ameland: Correlation Coefficients as function of elevation

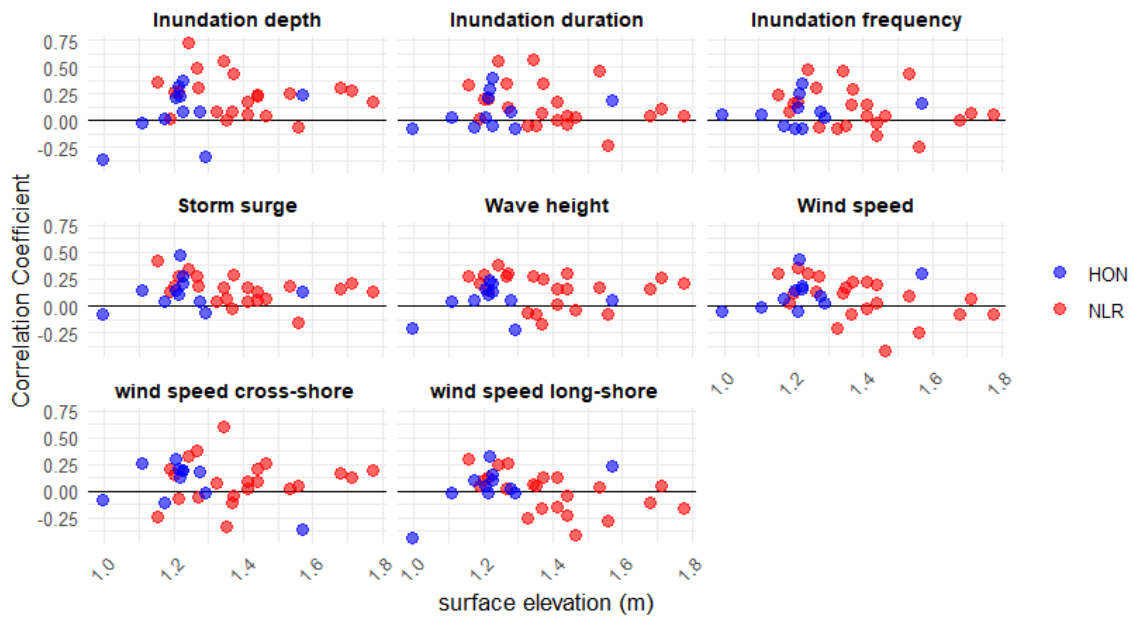


Figure 33: Correlation coefficients between accretion and storm variables on Ameland plotted as a function of surface elevation. Each panel has a different storm variable. The correlation coefficients are the same as presented in figure 8.

Ameland: Correlation Coefficients as function of vegetation height

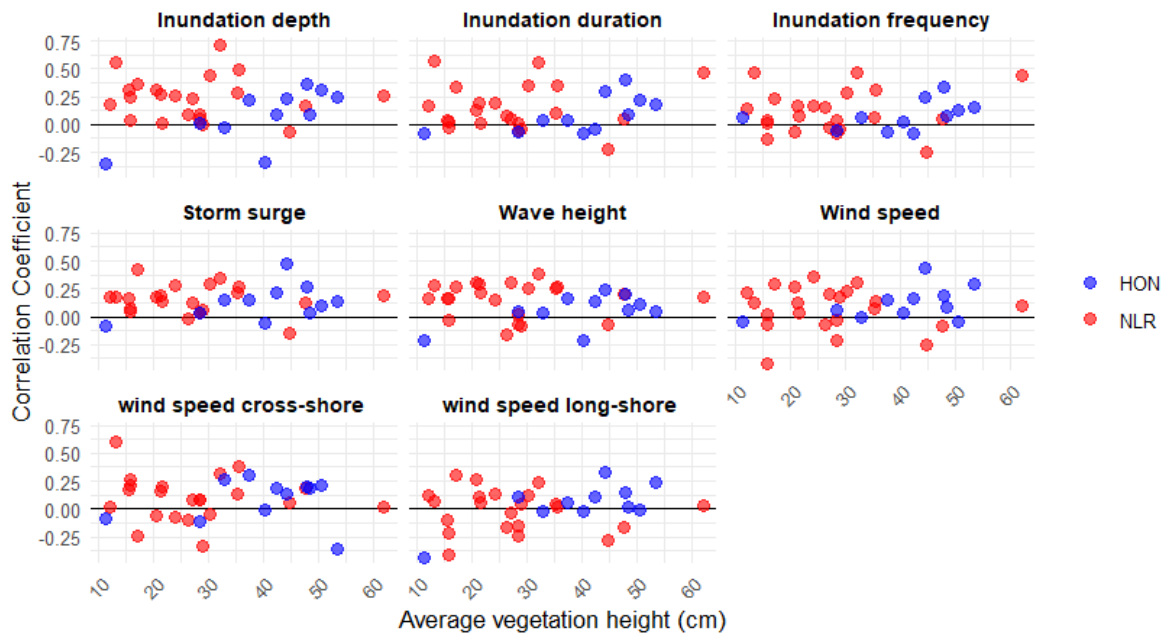


Figure 34: Correlation coefficients between accretion and storm variables on Ameland plotted as a function of average vegetation height. Each panel has a different storm variable. The correlation coefficients are the same as presented in figure 8.

Schiermonnikoog: Correlation Coefficients as function of distance to creek

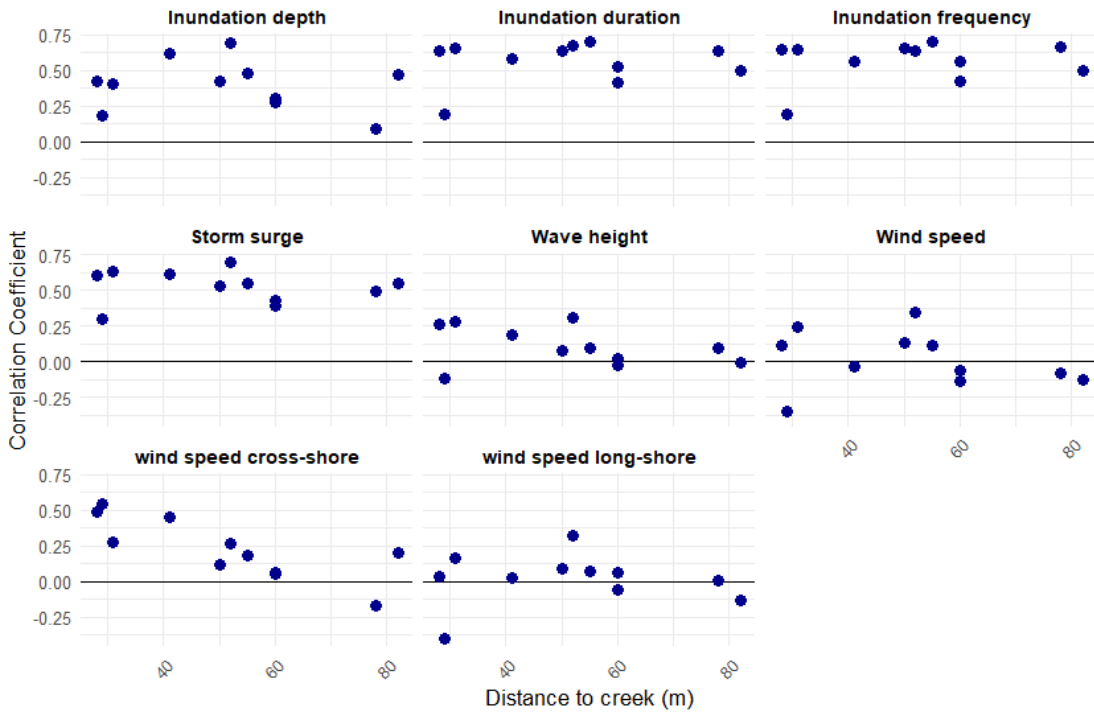


Figure 35: Correlation coefficients between accretion and storm variables on Schiermonnikoog plotted as a function of distance to creek. Each panel has a different storm variable. The correlation coefficients are the same as presented in figure 9.

Schiermonnikoog: Correlation Coefficients as function of distance to shoreline

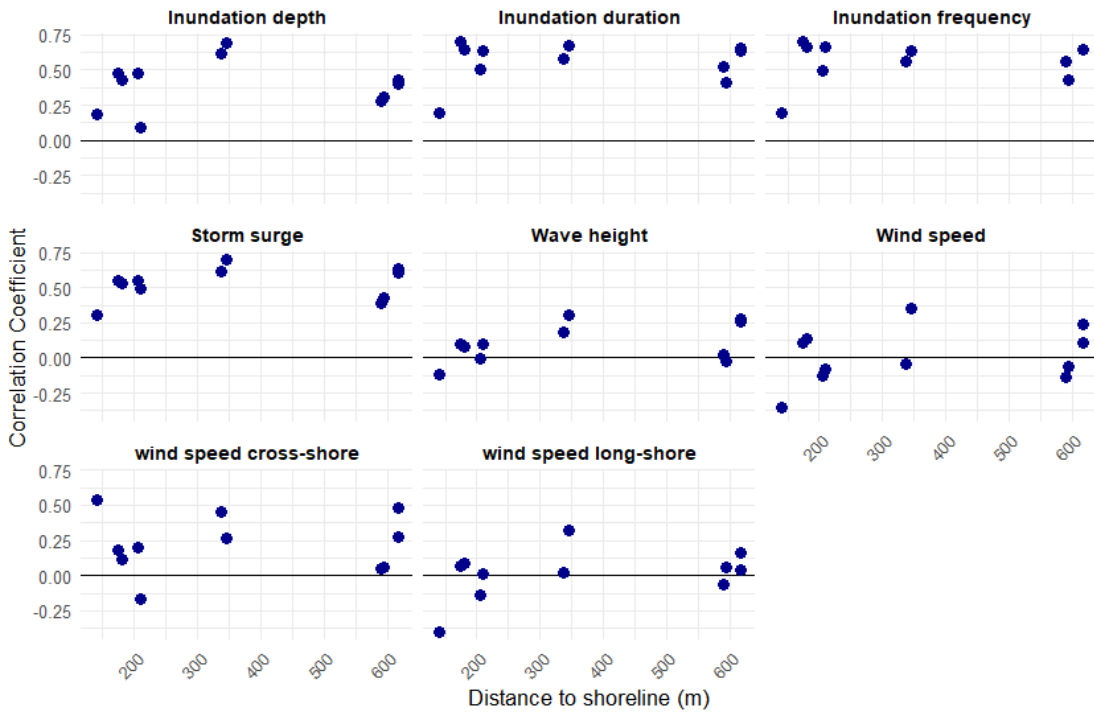


Figure 36: Correlation coefficients between accretion and storm variables on Schiermonnikoog plotted as a function of distance to shoreline. Each panel has a different storm variable. The correlation coefficients are the same as presented in figure 9.

Schiermonnikoog: Correlation Coefficients as function of distance to sediment source

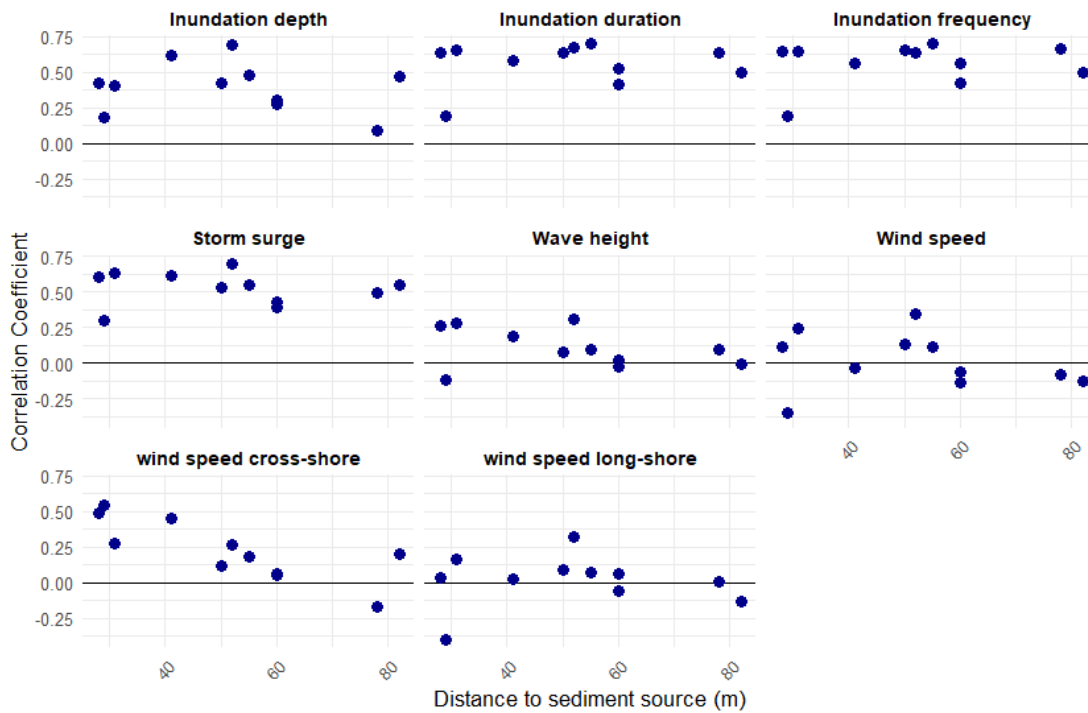


Figure 37: Correlation coefficients between accretion and storm variables on Schiermonnikoog plotted as a function of distance to sediment source. Each panel has a different storm variable. The correlation coefficients are the same as presented in figure 9.

Schiermonnikoog: Correlation Coefficients as function of elevation

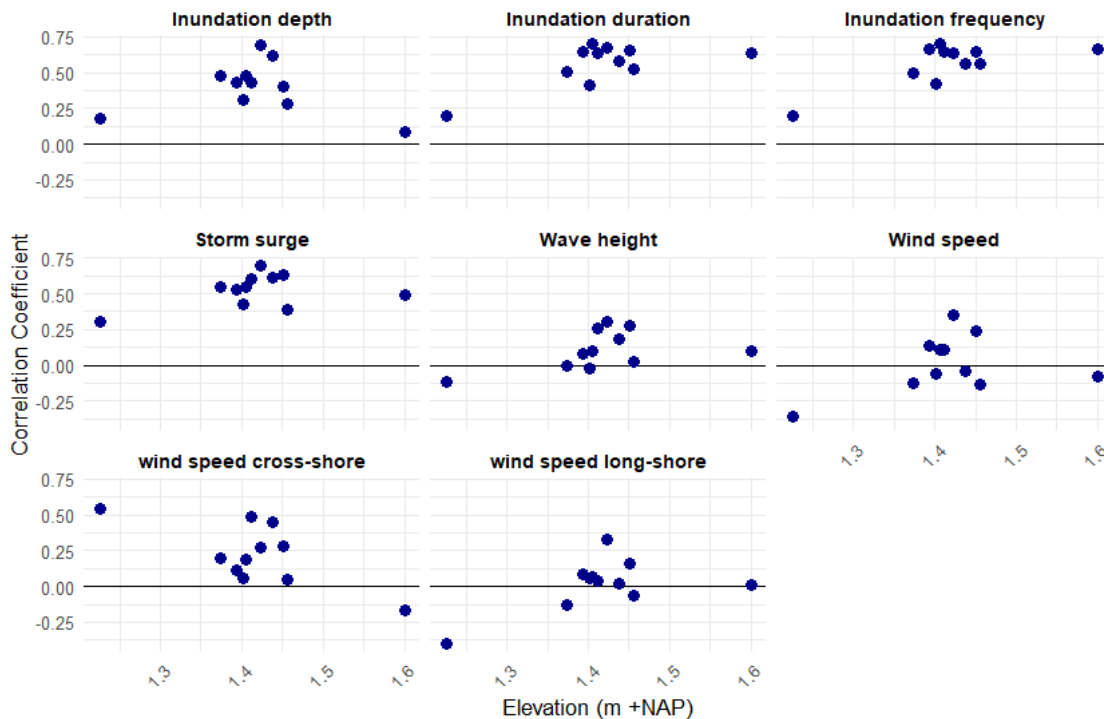


Figure 38: Correlation coefficients between accretion and storm variables on Schiermonnikoog plotted as a function of distance to elevation. Each panel has a different storm variable. The correlation coefficients are the same as presented in figure 9.